EXPERIMENTAL CHARACTERIZATION OF THERMOPHYSICAL PROPERTIES AND CONVECTIVE HEAT TRANSFER BEHAVIOR OF HEXAGONAL BORON NITRIDE NANOFLUIDS

by

Beybin İlhan

B.S., Mechanical Enginerring, Middle East Technical University, 2013

Submitted to the Institute for Graduate Studies in
Science and Engineering in partial fulfillment of
the requirements for the degree of
Master of Science

Graduate Program in Mechanical Engineering
Boğaziçi University

2016

EXPERIMENTAL CHARACTERIZATION OF THERMOPHYSICAL PROPERTIES AND CONVECTIVE HEAT TRANSFER BEHAVIOR OF HEXAGONAL BORON NITRIDE NANOFLUIDS

APPROVED BY:

Assoc. Prof. Hakan Ertürk (Thesis Supervisor)	.....
Assoc. Prof. Almıla Güvenç Yazıcıoğlu	.....
Assoc. Prof. Hasan Bedir	.....

DATE OF APPROVAL: 23.06.2016

to my beloved family...

ACKNOWLEDGEMENTS

First and foremost, I would like to express my greatest gratitude to my thesis supervisor Assoc. Prof. Hakan Ertürk for his endless support, guidance, motivation and immense knowledge. He has always been an inspiration to me even at the toughest times. He has encouraged me to not be afraid to ask questions every time and taught me how to approach problems with a scientific point of view. With his guidance, I have learned the virtue of questioning and joy of dedication to finding the answers.

Besides my advisor, I am grateful to my committee members Assoc. Prof. Almıla Güvenç Yazıcıoğlu and Assoc. Prof. Hasan Bedir for their time, insightful comments and constructive criticism for my study. I would specially like to say that Assoc. Prof. Almıla Güvenç Yazıcıoğlu has always been an inspiration figure for me since my undergraduate studies at METU. She has showed me the value of being a great academician and she always motivated me to pursue an academic career. I would also like to thank Assoc. Prof. Derek Baker from METU for supporting and encouraging me to find my potential in a scientific research career during my undergraduate years.

I would also like to thank my lab mates; Özgür Atik and Melike Kurt for their support and friendship, they helped me to overcome many problems that I encountered while experimenting. I am especially grateful to Gökçe Aköz, Elif Yılmaz and Onur Yüksel for their endless support, encouragement and love; their presence always reminded me how lucky I am to have them. I am also thankful to my dearest friends; Bahar Öner, Tuba Mumcu, Gülfem İnaner, Buse Altınel, Harika Duyu and Nazlı Turan for their valuable friendship and all the greatest times we have spent together.

Finally, I would like to thank my family, Düriye İlhan, Rifat İlhan and Serav İlhan. They have always believed in me and supported me at my each step.

This thesis has been supported by The Scientific and Technological Research Council of Turkey (TUBITAK), under the grant 111M177 of the 1001 Program.

ABSTRACT

EXPERIMENTAL CHARACTERIZATION OF THERMOPHYSICAL PROPERTIES AND CONVECTIVE HEAT TRANSFER BEHAVIOR OF HEXAGONAL BORON NITRIDE NANOFLUIDS

Hexagonal boron nitride (hBN) is a highly stable dielectric ceramic material that exhibits versatile properties such as, exceptionally high thermal conductivity and good chemical inertness. In this study, preparation, stability and thermophysical properties and convective heat transfer characteristics of hBN containing DI water, ethylene glycol (EG) and EG-DI water mixture (by volume 50%) based nanofluids are experimentally investigated. Well dispersed, stable nanofluids, containing hBN nanoparticles are produced with a two-step method. The stability is evaluated by quantitative methods such as, time dependent Zeta Potential, and thermal conductivity measurements. Morphological characterization is completed by qualitative methods such as, ESEM (Environmental Scanning Electron Microscopy) and TEM (Transmission Electron Microscopy). The thermal conductivity enhancement of nanofluids (vol. conc. range: 0.03-3%), is investigated in accordance with increase in viscosity. Thermally developing laminar forced convection of hBN-water nanofluids with a particle volume concentration range of 0.1-1% are considered for a Re range of 800-1700. It is observed that the hBN nanofluids have remarkably higher thermal conductivity values than their corresponding base fluids. Moreover, hBN-water nanofluids with relatively dilute particle suspensions, exhibit significant increase in thermal conductivity with respect to the viscosity increase. For the case of convective heat transfer behavior, the enhancement in the convective heat transfer coefficient of nanofluids is proportional to the observed thermal conductivity enhancement. Therefore, there is no abnormal enhancement in the measured Nusselt number, and measured values are in good agreement with predictions by standard laminar thermally developing flow correlations.

ÖZET

HEKZAGONAL BOR NİTRÜR NANOAKIŞKANLARININ TERMOFİZİKSEL ÖZELLİKLERİNİN VE TAŞINIM ISI TRANSFERİ KARAKTERİSTİKLERİNİN DENEYSEL OLARAK İNCELENMESİ

Hekzagonal bor nitrür (hBN), yüksek ısıl iletim katsayısı ve üstün kimyasal inertlik gibi çok yönlü özellikleri olan, yüksek seviyede kararlı ve yalıtkan bir seramik malzemedir. Bu çalışmada hBN nanparçacıkları içeren iyondan arındırılmış su, etilen glikol (EG) ve EG-su (%50 hacimsel oran) baz sıvılı nanoakışkanların, hazırlanması, kararlılığı, termofiziksel özellikleri ve taşınım ısı transferi karakteristikleri deneysel olarak incelenmiştir. Bu sebeple, hBN nanoparçacıkları içeren kararlı nanoakışkanlar 2 adımlı üretim yöntemiyle üretilmiştir. Nanoakışkanların kararlılığı, zamana bağlı Zeta Potansiyel ve ısıl iletkenlik ölçümleri ile niceliksel olarak belirlenmiştir. Morfolojik karakterizasyon ise çevresel tarayan elektron mikroskobu (ESEM) ve zamana bağlı, tarayan elektron mikroskobu (TEM) ile tamamlanmıştır. %0.03 ile %3 arasında hacimsel konsantrasyonlu nanoakışkanların ısıl iletkenlik katsayısı artırımları, vizkozite değişimleri ile koordine olarak gözlemlenmiştir. hBN nanoakışkanlarının taşınım ısı transferi özellikleri, ısısal olarak gelişen katmanlı akışlarda, hacimsel oranı %0.1 ile %1 arasında değişen hBN-su nanoakışkanları, 800 ile 1700 Re arasındaki boru içi zorlanan akışlarda incelenmiştir. hBN nanoakışkanlarının, dikkat çekici ölçüde yüksek ısıl iletkenlik katsayısına sahip oldukları gözlemlenmiş olup, ayrıca, hBN-su nanoakışkanları, görece düşük konsantrasyonlarda bile, vizkozite değerlerindeki artışa kıyasla, önemli ölçüde artışı ısıl iletkenlik katsayısında göstermiştir. Taşınım ile ısı transferi özellikleri bakımından hBN-su nanoakışkanları, ısıl iletkenlik artışına parallel bir artış göstermiştir. Bu yüzden Nusselt sayısında normalin dışında bir artış görülmemiş olup, elde edilen bulgular katmanlı akışlar için standart sayılan ısıl yönden gelişen akış korelasyonlarından elde edilen sonuçlar ile uyumludur.

TABLE OF CONTENTS

LIST OF FIGURES

LIST OF TABLES

LIST OF SYMBOLS

C	Celsius
c_p	Heat capacity of fluid
d_p	Diameter of nanoparticles
D	Diameter of the pipe
h_x	Local heat transfer coefficient
K	Kelvin
k_{bf}	Thermal conductivity of base fluid
k_f	Thermal conductivity of fluid medium
k_{nf}	Thermal conductivity of nanofluid
k_p	Thermal conductivity of nanoparticle
l	Length of the pipe
k_p	Thermal conductivity of nanoparticle
M	Molecular weight
$\dot{m}$	Thermal conductivity of nanoparticle
mm	Milimeter
N	Avagadro number
n	Shape Factor for Hamilton and Crosser model
nm	Nanometer
Nu_x	Local Nusselt number
Pr	Prandtl number
q'	Heat per length of the wire
q"	Surface heat flux around the tube
Re	Reynolds number
rpm	Revolutions per minute
T_0	Initial temperature of the medium
$T_{m,i}$	Inlet mean temperature
$T_{m,o}$	Outlet mean temperature
$T_{m,x}$	Local mean temperature

$T_{s,x}$	Local surface temperature
V_f	Volume flow rate
W	Watt
x	Position along the pipe
α_f	Thermal diffusivity of fluid
ΔT	Transient temperature change
$\varphi[\%]$	Percent volume concentration
Ψ	Sphericity factor for Hamilton and Crosser model
$\Psi[\%]$	Percent weight concentration
μ_{bf}	Dynamic viscosity of base fluid
μ_{nf}	Dynamic viscosity of nanofluid
μ_{bf}	Dynamic viscosity of surfactant fluid
π	Pi number
σ_h	Uncertainty of convective heat transfer coeff.
σ_{Nu}	Uncertainty of Nusselt number
ρ	Density
ρ_p	Density of particle
ρ_{bf}	Density of base fluid
ρ_{sf}	Density of nanofluid

LIST OF ACRONYMS/ABBREVIATIONS

BN	Boron nitride
BNNS	Boron nitride nanosphere
BNNT	Boron nitride nanotube
CNT	Carbon nanotube
CTAB	Cetyl trimethylammonium bromide
DI	De-ionized
DLS	Dynamic light scattering
DWNTs	Double walled nanotubes
EG	Ethylene glycol
ESEM	Environmental scanning electron microscopy
GO	Graphene oxide
hBN	Hexagonal boron nitride
HCTAB	Hexadecly trimethylammonium bromide
MO	Mineral oil
MWNTs	Multi walled nanotubes
PAO	Polyalpha olefin oil
PDDA	Polydiallyldimethylammonium chloride
PVP	Polyvinyl pyrrolidone
SDBS	Sodium dodecyl benzene sulfonate
SDS	Sodium dodecyl sulfate
SEM	Scanning electron microscopy
STEM	Scanning transmission electron microscopy
TEM	Transmission electron microscopy

1. INTRODUCTION

1.1. Problem Overview

Within the progress of applications of thermal sciences, many efforts and improvements have been devoted to heat transfer enhancement area to improve systems' efficiency. Due to increase in the thermal loads caused by more power demand and smaller feature sizes for the products, cooling has become one of the important challenges within the application areas such as manufacturing, transportation industry, chip or package level liquid cooling and energy supply industry. The conventional ways to improve heat transfer characteristics in thermal systems can be subgrouped as; increasing the heat transfer surface area or flow velocity, and dispersing the solid particle additives in heat transfer fluids. Considering these conventional ways; introducing milllimeter or micrometer sized particles in heat transfer fluids for improvement is actually a relatively old technique to improve heat transfer rates. The major problem with this method is the rapid settling of the particles sustained within the engineered fluids. This method would also cause wearing of the materials they have been circulating in, clogging of channels, undesired pressure drop and greater pumping power. Another way of increasing heat transfer characteristics is using the extended surface areas as stated above. Considering the fact that current designs of thermal management systems have reached the size limitations of these extended surfaces, this method is not highly adoptable to the new technologies such as micro scale heat exchangers and microchannels.

In the light of the stated reasonings above, the conventional ways are not well-responding to the intensified need for more efficient ways of heat transfer. For that reason new engineered heat transfer fluids are required as a new approach to meet the increasing demand for more efficient heat transfer fluids in many industries. Considering the fact that dispersing solid additives to the heat transfer fluids can improve heat transfer characteristics of fluids compared to the base fluid, Choi (1995) introduced the novel concept of nanofluids, meaning of colloidal suspensions with nanometer sized particles dispersed in base fluids. Keeping in mind that mechanical, optical, electrical, magnetic and thermal properties of nanoparticles are superior than those of bulk materials, nanofluids are

considered to be as an important opportunity to apply nanotechnology to thermal engineering. A general statement can be made as, nanofluids are believed to be the next generation heat transfer fluids.

Regarding the fact that the concept of nanofluids is a newly emerged research area, there exist several challenges in terms of implementation of nanofluids to the industrial applications. The first and the most important problem is the stability issue which will also cause problems for the long term usage. There have been various methods to improve the long term stability of nanofluids within the literature. The implementation of such methods at the preparation stage of nanofluids has a major importance to eliminate the problem of instability caused by sedimentation. Another drawback is the viscosity increment of the nanofluids which will also cause higher pumping power requirement for the heat transfer systems. In addition to these challenges, it should be noted that there is a lack of consensus among the data provided by various research groups in the literature which would make it hard to obtain a standardized level of production for nanofluids.

1.2. Literature Survey

Heat transfer enhancement has been the interest of scientists and engineers not only for designing high efficiency systems, but also sustaining safe operation of devices and systems Using advanced materials with improved properties has been one of the most widely adopted approaches of heat transfer enhancement. While the common heat transfer fluids, such as water, engine oil or ethylene glycol have limited heat transfer capacities based on their thermophysical properties; enhancing heat transfer is possible by utilizing heat transfer fluids with improved properties. Employing solid additives to increase the transport and heat transfer characteristics of liquids, is a well-known method (Ahuja, 1975; Sohn *et al.*, 1981). Prior studies related to heat transfer fluids with dispersed millimeter or micrometer sized particles demonstrated that heat transfer characteristics can be improved. However, application of these suspensions is not practical due to inevitable problems such as rapid coagulation and sedimentation. Dispersed micro or millimeter sized particulate suspensions show very poor stability as particulates settle rapidly and their use might lead to clogging in channels, agile wearing of materials caused by abrasive action of particles and significant increase in pressure drop (Das et al., 2006, Chandrasekar et al., 2010).

Nanofluids are relatively new class of engineered liquids comprised of dispersed nanoparticles with at least one dimension less than 100 nm and they have been a subject of great interest since their introduction by Choi (1995) due to their potential to improve heat transfer. Colloidal suspensions of nanoparticles, are expected to possess higher thermal conductivity, better long term stability and cause less pressure drop than suspensions of larger particles (Das *et al*., 2006). Considering the fact that at nanoscale, as the percentage of atoms at the surface of a material becomes significant, material properties are different than the coarse grain structured bulk materials' properties (Das *et al*., 2007). In order to provide stability within the nanofluid, the agglomeration of nanoparticles must be prevented.

1.2.1. Nanofluid Preparation and Stability Improvement Methods

There are two main methods to disperse and homogenize nanoparticles into base fluids to prepare nanofluids. The first method is the single step method in which nanoparticles and nanofluid are produced on a single process. The most important advantage of this method is that the stability problems are minimized due to concurrent production of nanoparticles and nanofluids at once . On the other hand this is generally a costly method with major drawbacks on the implementation to the industry and mass production.

The most frequently adopted method of nanofluid production is the two step method. Although this method enables relatively easier industrial implementation and mass production, achieving stable dispersions can be problematic as agglomerations are easily formed due to nanoparticles' high surface energy and strong van der Waals forces between nanoparticles (Wong and Castillo, 2010). Heat transfer properties could change in time with a considerable uncertainty due to these stability problems. Therefore, long term stability is considered as the key issue in nanofluids' practical applications and additional treatments are applied to these suspensions to prevent rapid coagulation and sedimentation of nanoparticles. Methods such as ultrasonic mixing, pH control and surfactant additives are used during the preparation of nanofluids in order to attain well dispersed suspensions, and long term stability (Ghadimi *et al.*, 2011). The dispersion quality is highly dependent

on the nature of nanoparticles in terms of particle size, morphology, concentration, and their respective interactions with the base fluid. Therefore, a specific combination of such treatments should be implemented at production stage of a specific nanofluid (Chou *et al.*, 2005; Huang *et al.*, 2009). The level of stability can be defined based on different metrics such as observing the change in mean aggregate size, zeta potential, or change in the transport properties along time (Wang *et al.*, 2008, Chou *et al.*, 2005; Lee *et al.*, 2006).

Ultrasonication is the most widely utilized process in the literature to increase the stability of nanofluids. When a colloidal nanofluid suspension is exposed to ultrasonic vibration via a vibrating probe placed in the medium, low pressure field is generated around the ultrasonic probe and the fluid begins to move. At sufficiently high frequencies, this movement ceases and vibration of fluid molecules emerge which leads to formation of vacuum bubbles and microscopic shock waves within the fluid. These shock waves fade within microseconds, but a large amount of energy release occurs, leading to breakage of large agglomerates within the colloidal suspensions of nanofluids(Perez *et al.* 2004) Although it is considered as the essential process for 2 step production of nanofluids, no standardization has been established for duration and power amplitude applied for this process. If the suspension is not sonicated for sufficient time to reduce the nanoparticle agglomerate size, instability within the nanofluid is unavoidable. On the other hand, if the suspension is sonicated too long, fragmentized nanoparticles can re-agglomerate due to the effect of high surface energy. Thus, an optimal sonication time needs to be determined to achieve optimal agglomeration size and stability for different combinations of nanoparticle, base fluid, and particle volume concentration (Ghadimi *et al.*, 2011). Patel *et al.* (2005) observed that 11 nm sized, 0.8% by volume Al_2O_3 nanoparticles dispersed in water, can be stabilized with 6 hours of sonication. Das *et al.* (2003) reported that after sonicating Al_2O_3 and CuO nanofluids for 12 hours, no sedimentation was observed within the first 12 hours for %1, %2, %3, 4% volume concentrations. After 12 hours, minor sedimentation was observed in %3 and 4% volume concentrations. Assael *et al.* (2005) investigated the effect of ultrasonic homogenization time of water based C-MWNTs and C-DWNTs. They found out that nanofluids prepared with commercial surfactant, Cetyl Trimethyl Ammonium Bromide (CTAB), exhibited stable dispersions when an ultrasonic treatment between 30-60 minutes is applied. They have claimed that smaller or larger sonication durations can cause rapid precipitation of nanoparticles for the specified

nanofluids. Yang *et al.* (2006) investigated the effect of ultrasonication on the size of the agglomerated particles in CNT-oil nanofluids and concluded that higher sonication time and power levels resulted in smaller clusters.

The use of surface active materials or surfactants is another widely adopted method for achieving stable suspensions (Xua and Lie, 2013; Yu *et al.*, 2012; Ghadimi and Metselaar, 2013). Surfactants for polar solvents consist of a hydrophobic tail portion and a hydrophilic polar head group. These two opposing forces control the self-association process with tail–water interactions. In aqueous phase, hydrophobic tail portion constitutes the core portion of the aggregates forming micelles, where the hydrophilic head portion are in contact with the enclosing liquid medium creating a level of continuity between nanoparticles and base fluid (Yu and Xie., 2012). Surfactant reagents can remarkably affect the surface characteristics of particulates even when small amounts are used. However, use of such a third agent also leads to an increase in base fluid viscosity (Studart *et al.*, 2007). Moreover, attachment of the surfactant molecules on the surfaces of nanoparticles may also act as an additional thermal resistance between the nanoparticles and the base fluid, limiting the enhancement in effective thermal conductivity. Therefore, the amount of surfactant used is a key parameter for achieving well dispersed nanofluids, and optimum amount of surfactant material should be identified in order to maximize the benefit. There are several studies observing the effect of using surfactants for nanofluid systems. Zhou *et al.* (2012) studied two different kinds of surfactants, SDS and PVP, dispersed in water and showed that the amount of surfactant material has a significant effect on base fluid viscosity and thermal conductivity. Xuan *et al.* (2013) investigated the effect of SDBS on Cu-water nanofluids' thermal performance, and claimed that SDBS has negative effect on heat transfer characteristics of the liquid media and enhancements are suppressed with surfactant usage. They have attributed that to oversaturation of SDBS causing excessive surfactant layering on the nanoparticles.

1.2.2. Thermal Conductivity Enhancement of Nanofluids

There are many experimental and theoretical studies investigating the thermal conductivity of nanofluids. While some studies in recent literature report anomalous increase in thermal conductivity beyond the predictions of effective medium theories, there

are other studies reporting thermal conductivity increase similar to or less than these predictions.

One of the conventional one is the Maxwell's effective medium theory (Maxwell, 1881). According to Maxwell, suspensions with spherical solid particles dispersed in, are expected to have an effective thermal conductivity of;

$$\frac{k_{nf}}{k_{bf}} = \frac{k_p + 2k_{bf} + 2\varphi(k_p - k_{bf})}{k_p + 2k_{bf} - \varphi(k_p - k_{bf})} \tag{1.1}$$

where k_{nf}, k_{bf} and k_p corresponds to; thermal conductivities of nanofluid, base fluid, and particle respectively, and φ denotes the volume concentration of particles within the suspension.

As an improved version of Maxwell model to predict the effective thermal conductivity of spherical solid-fluid mixtures without particle concentration limitation within the fluid was proposed by Bruggeman (1935).

$$\varphi\left(\frac{k_p - k_{nf}}{k_p + 2k_{nf}}\right) + (1-\varphi)\left(\frac{k_{bf} - k_{nf}}{k_{bf} + 2k_{nf}}\right) = 0 \tag{1.2}$$

Considering the fact that thermal conductivity increase cannot be solely attributed to particle concentration within the liquid media, another model for solid-liquid mixtures' thermal conductivity prediction is developed by Hamilton and Crosser (1962) for non-spherical particles.

$$\frac{k_{nf}}{k_{bf}} = \frac{k_p + (n-1)k_{bf} - (n-1)(k_{bf} - k_p)\varphi}{k_p + (n-1)k_{bf} + (k_{bf} - k_p)\varphi} \tag{1.3}$$

where n denotes the shape factor of the particles and defined as $n=\Psi/3$. Ψ is the sphericity factor . Hamilton Crosser model is an extension of Maxwell's theory, accounting for the nonsphericity of the particles. Spherical particles have a sphericity $\Psi=1$, leading a shape factor of n=3.

Although conventional models may provide reasonable predictions for solid-liquid mixtures with relatively larger particles, there are many experimental results stating that the thermal conductivity enhancement is dependent on several more parameters and enhancement is beyond the predictions of effective medium theories.

1.2.2.1. Experimental Results. Eastman *et al.* (1996) prepared CuO-DI water nanofluids with 36 nm particles and reported 60% thermal conductivity enhancement for 5% nanoparticles by volume. Lee *et al.* (1999) investigated CuO-EG nanofluids and claimed that nanofluids with 4% particle loading by volume resulted in 20% thermal conductivity increase. Nikkam *et al.* (2014) prepared Cu-diethylene glycol nanofluids with one step method and observed 7.2% thermal conductivity enhancement for the nanofluids with 1.6% particle weight fraction, while viscosity increases by 5.2%. Xie *et al.* (2001) worked with 25 nm SiC particles to prepare water based nanofluids and observed 15.8% thermal conductivity increase for 4.2% particle loading by volume. Timofeeva *et al.* (2007) investigated thermal conductivity and viscosity increase in Al_2O_3-water and EG nanofluids, and reported that both thermal conductivity and viscosity increase are within the range predicted by effective medium theories. Chandrasekar *et al.* (2010) observed the thermal conductivity and viscosity increase of Al_2O_3-water nanofluids in the particle volume concentration range of 0.33-5%. They reported that viscosity increase is notably higher than that of thermal conductivity; at a particle volume concentration of 3% thermal conductivity increase is reported to be ~9%, whereas viscosity increase reaches up to ~45%. Buongiorno *et al.* (2009) tested nanofluids with aqueous and non-aqueous basefluids, metal and metal oxide particles, near-spherical and elongated particles, at different concentrations. They also stated that thermal conductivity enhancement is in good agreement with predictions of effective medium theories.

Many research groups have reported that nanofluids exhibit remarkable thermal conductivity enhancements even for relatively low particle loadings (Murshed and Castro, 2014; Liu *et al.*, 2006). Wen and Ding (2004) investigated the thermal conductivity enhancement of CNT-DI water nanofluids with 0.84% particle weight concentration at 20 and 45^{o}C and reported an enhancement of 23.7 and 31%, respectively. Wang *et al.* (2012) prepared EG, poly alpha olefin oil (PAO), and water based graphite nanofluids, and

reported that at 1% particle volume concentration, thermal conductivity increases 153, 201 and 113%, respectively.

1.2.2.2. Enhancement Mechanisms. There are several theories explaining the conductivity enhancement beyond predictions of effective medium theories. Jang *et al.* (2004) and Prasher *et al.* (2005) suggest that Brownian motion of nanoparticles within the fluid creates micro-convection effects, enhancing the energy transfer. Eapen *et al.* (2007), Keblinski *et al*. (2002), stated that nanoparticle agglomerations can create paths for efficient energy transport due to percolation. Eapen *et al.* (2007) proposed that there exists a highly-ordered liquid layer with relatively higher conductivity, referred as the nano-layer, surrounding nanoparticles increasing the energy transfer rate. Keblinski *et al.* (2002) investigated the possible enhancement reasons for anomalous increases in nanofluids' thermal conductivity and indicated that such behavior can be attributed to cluster effective paths, enabling enhanced heat conduction. Karthikeyan *et al.* (2008) investigated the possible mechanisms for thermal conductivity enhancement for CuO containing water and EG based nanofluids. They reported that the enhancement in thermal conductivity is mainly due to smaller particle size and monodispersity of particles. Gao *et al.* (2009) investigated the effect of clustering formations in thermal conductivity and concluded that Brownian motion is not the key factor for thermal conductivity increase in Alumina-hexadecane nanofluids. They have tested different phases of nanofluids including frozen, liquid and hot fog to underline the temperature effect and identify Brownian motion's contribution to the heat transfer enhancement, and they stated that local clustering is the dominant mechanism behind conductivity increase. Baby *et al.* (2011) reported that hydrogen exfoliated graphene nanoparticles have remarkable effect on nanofluids' thermal conductivity enhancement at relatively low concentrations. Their study considers graphene-water and EG nanofluids' in a temperature range of 25-50^{o}C. They observed a thermal conductivity increase up to 14% for water based nanofluids with 0.056% particle volume concentration at 25^{o}C for. However, only 3-4% enhancement was observed for 0.05% particle volume concentration graphene-EG nanofluid. Considering that thermal conductivity enhancement reaches 60% at 50^{o}C for water based nanofluids, they claimed that the dominant enhancement mechanism was Brownian motion of nanoparticles. Wang *et al.* (2012) investigated the effects of heat conduction mechanisms and observed that for graphite nanoflake containing nanofluids, thermal conductivity increases remarkably as percolating structures are formed.

They have also observed a nonlinear behavior of thermal conductivity increase, where it increases suddenly with increasing graphite volume concentration and graphite nanoflakes form clusters. However, the increase slows down with further increase in volume concentration, and a sharp change in the rate of increase is observed as nanofluid reaches the percolation threshold. After percolation threshold, the bonding between graphite nanoflakes becomes weaker leading to separation in flakes resulting in an interface resistance with slower thermal conductivity increase rate. Zhu *et al.* (2006) observed a similar behavior with aqueous Fe_3O_4 nanofluids demonstrating a nonlinear thermal conductivity enhancement with sharper increase at relatively lower particle loadings. They attributed the decrease in the enhancement slope after a certain volume concentration to higher concentrated nanofluids having more populated, relatively more dense and compact clusters. They stated that at low volume concentrations loosely packed clusters are formed leading to an increase in the number of heat transfer paths, whereas increasing the particle concentration further just increases the density of existing paths rather than creating new ones.

1.2.3. Rheological Behavior and Viscosity Change of Nanofluids

Another aspect that should be considered is the rheological behavior and viscosity change of nanofluids. It is well known that the addition of nanoparticles into a fluid can substantially change the rheological properties and understanding these changes is also crucial as nanofluids are considered as an alternative for current heat transfer fluids. While the heat transfer capacity can be increased by thermal conductivity enhancement, similar increase can also be observed for viscosity. The power required to pump a fluid at a given flow rate is expected to increase as the viscosity increases. Therefore, depending on the system features, a reduction of flow velocity could result in suppressing the benefit of thermal conductivity enhancement and limit heat transfer characteristics.

First conventional model to formulate the effective viscosity of solid-liquid mixtures with spherical particles was proposed by Einstein (1905).

$$\mu_{nf} = (1 + 2.5\varphi)\mu_{bf} \tag{1.4}$$

where μ_{nf} and μ_{bf} is the viscosities of the solid-liquid mixture and the base fluid respectively. According to Einstein's theory, the effective viscosity of the suspension is linearly dependent only on volumetric particle concentration.

Another model is stated by Brinkman (1947) and it suggests that effective viscosity can be defined as the power of volume concentration.

$$\mu_{nf} = \left(\frac{1}{1-\varphi^{2.5}} \right) \mu_{bf} \tag{1.5}$$

Besides from the conventional theoretical models, that are applicable to particle volume concentrations of 0-2%, Corcione (2011) developed empirical model by using a large number of experimental data for predicting the dynamic viscosity.

$$\mu_{nf} = \left(\frac{1}{1-\varphi^{2.5}} \right) \mu_{bf} \tag{1.6}$$

where d_f is the equivalent diameter of a base fluid molecule, defined as,

$$d_f = \left(\frac{6M}{N\pi\rho_{f0}} \right)^{1/3} \tag{1.7}$$

in which M is the molecular weight of the base fluid, N is the Avagadro number and ρ_{f0} is the mass density of the base fluid calculated at temperature of T_0=293 K. One of the advantages of Corcione model is that, it includes the effect of base fluid type on the change of viscosity.

Different research groups have observed different behavior in viscosity increase and rheological characteristics with different base fluids and nanoparticle additives (Murshed *et al.*, 2008; Wang and Mujumdar, 2008). A brief summary of studies regarding the rheological behavior and viscosity change is presented in Table 1.1. In accordance with the wide range of reported studies, the increase ratios cannot be well predicted by classical models in most cases. The results indicate that several different parameters, such

as particle size and shape, temperature of the medium, ordering and the dispersion state of the nanoparticles, specific interface interactions between nanoparticles and base fluids, and dispersion quality have significant effect on the viscosity change.

Table 1.1. A brief summary of rheological studies about nanofluids in the literature.

Researcher	**Nanofluid**	**Behavior**	**Viscosity Increase**
Chen *et al.* (2007)	TiO_2- EG	Newtonian	10% for 1% vol. conc.
Murshed *et al.* (2007)	Al_2O_3-water	Newtonian	24% for 1% vol. conc.
Guo *et al.* (2015)	BN/EG	-	47% for 3% vol. conc.
Zyla *et al.* (2015)	BN/EG	Non-Newtonian/ Shear Thinning	-
Tijerina *et al.* (2012)	hBN-MO	Newtonian	-
Sleiti *et al.* (2011)	hBN-PAO	Newtonian	-
Prasher *et al.* (2006)	Al_2O_3-PG	Newtonian	-

There is a lack of agreement in the reported thermophysical data presented by different research groups working with similar particles and base fluids. These differences can be attributed to a number of factors such as variations in particle size and shape, surfactants used, resulting changes in the mean size of aggregates, level of sedimentation. While lack of detailed information about preparation methods makes it hard to interpret such differences, there is a need for further experimental studies for characterization of different nanofluids.

1.2.4. Boron Nitride

Boron nitride (BN) is a ceramic material that exists in different crystal structures similar to carbon. The hexagonal form of BN, hBN, is the softest among the other polymorphs of BN and has a similar structure to graphite. Due to its chemical inertness and high in-plane thermal conductivity, it can be considered as a promising candidate material for heat transfer fluids. BN and hBN nanofluids have been introduced recently as heat transfer and lubrication fluids (Tijerina *et al.*, 2012; Sahoo and Das, 2013; Guo *et al.*, 2015; Mohan *et al.* 2015; Zyla *et al.*, 2015). While there is still very limited data in the literature regarding the hBN nanofluids, there are reported issues concerning their stability, thermal conductivity and rheological behavior. Guo *et al.* (2015) investigated the effect of several different surfactants on the stability of BN-EG nanofluids and reported that using PVP as a reagent resulted in better long term stability for nanofluids with surfactant weight fractions up to 10%. Tijerina *et al.* (2013) investigated nanofluids with two dimensional hBN nanoflakes produced with one step method, for lubrication and metal cutting applications and found that even small amounts of hBN fillers may reduce the contact friction with small viscosity increase and large enhancement in thermal conductivity. They also claimed that using small amounts of hBN fillers can lead to remarkable thermal conductivity increase with respect to the specified base fluid, mineral oil (MO). Another study by Sleiti (2012) reported that Newtonian behavior has been observed for hBN-PAO nanofluids with 0.25, 0.6 and 1% particle volume concentration at a temperature range -20 to 70 ^{o}C. Li *et al.* (2011) compared the thermal conductivities of 2 different BN-EG nanofluids containing 70 and 140 nm sized BN particles and observed that nanofluids with larger sized nanoparticles, resulted in higher thermal conductivity increase, compared to the ones prepared with smaller sized particles. The observed behavior was ascribed to the different shapes of BN nanoparticles and their specific surface area. They also observed that BN/EG nanofluids with 0.025% particle volume concentration have higher thermal conductivity enhancement compared to higher particle loadings. They claimed that at such relatively low concentration, chain-like loose aggregation of dispersed nanoparticles emerge and such morphology act as three dimensional dense network for heat transfer, whereas other presented concentrations demonstrated cloud-like compact morphology. Zhi *et al.* (2011) observed effects of using BN nanotubes and BN nanospheres on enhancing thermal conductivity and viscosity on water based nanofluids. They concluded BN nanotubes resulted in remarkably higher thermal conductivity increase whereas, BN nanospheres can keep viscosity relatively lower. They claimed that an optimal increase in

thermal conductivity accompanying a reasonable amount of viscosity increase can be achieved by using a mixture of BNNT and BNs nanoparticles together. Zyla *et al.* (2015) investigated the rheological profile of BN-EG nanofluids with 5 to 20% particle weight fractions. They focused on viscoelastic properties and studied viscosity and flow curves under different shear rates for materials and also viscosity increase under different temperature ranges. They presented that, there is no linear viscoelastic range and BN-EG nanofluids exhibit pseudoplastic, shear-thinning non-Newtonian behavior. Sahoo *et al.* (2013) prepared water based BN nanofluids with different surfactants, SDS, CTAB and Sodium HexaMeta Phosphate (SHMP) to investigate the wear and tribological behavior. They found that that use of dispersant agents has significant effect on particle size and tribological behavior of nanofluids. Using SDS with water based nanofluids resulted in smaller particle size and almost five times smaller coefficient of friction.

1.2.5. Convective Heat Transfer Behavior of Nanofluids

There are many experimental studies, focusing not only on the change in thermophysical properties, but also on characterization of the convective heat transfer behavior of nanofluids. Wen and Ding (2004) investigated Al_2O_3-water nanofluids under laminar flow and concluded that there is a significant enhancement in the entrance region and the enhancement decreases along the axial direction. Rea *et al.* (2009) studied Al_2O_3 water nanofluids under laminar flow, and reported that enhancement in convective heat transfer coefficient is more distinct at the fully developed region. However, the observed enhancement in the fully developed region cannot be identified as anomalous considering the measurement limits. Convective heat transfer characteristics of propanol nanofluids containing Al_2O_3, was investigated by Sommer and Yerkes (2010), within a large Reynolds number range. For Reynolds numbers between the range of 1000-2800, they reported that there is no abnormal enhancement beyond the thermophysical property increase. However, beyond Reynolds number of 2800, they observed decrease in convective heat transfer rate. Ding *et al.* (2006) reported a significant heat transfer coefficient increase, up to 350% at Re= 800, for multi walled carbon nanotube (MwCNT)-water nanofluids, in laminar flow regime and claimed that convective heat transfer enhancement was dependent on the axial direction on the test section Hwang *et al.* (2009) studied Al_2O_3-water nanofluids in laminar flow and reported that the enhancement in

convective heat transfer coefficient was beyond the increase in thermal conductivity enhancement and measured quantities cannot be predicted by standard theoretical correlations.

Baby and Ramaprabhu (2011) investigated thermophysical properties and convective heat transfer characteristics of the hydrogen exfoliated graphene containing nanofluids with two different base fluids, DI water and ethylene glycol (EG). They observed drastically larger enhancement in convective heat transfer compared to that of thermal conductivity. Wang *et al.* (2013) observed CNT-water nanofluids under laminar flow regime and found that heat transfer enhancement reached up to 190% for a volume concentration of 0.24% at a Reynolds number of 120. They observed that enhancement in convective heat transfer behavior was far more than the increase in thermal conductivity and the increase in pumping power very small, making them candidates for potential applications. Convective heat transfer characteristics of graphene–water nanofluid in laminar flow was investigated by Zanjani *et al.*(2016). They found 14.2% enhancement in convection heat transfer coefficient, where the thermal conductivity enhancement was 10.3% for a volume concentration of 0.02% at a Reynolds number of 1850. Hemmat *et al.* (2014) investigated, double-walled CNT-water nanofluids in turbulent flow in a double tube heat exchanger. They stated that even with the small amount of particle loadings such as 0.4% volume concentration, heat transfer enhancement reached up to 32% with 20% increase in pressure drop. Rayatzadeh *et al.* (2013) studied the effect of continuous ultrasonic mixing within the reservoir on convective heat transfer and pressure drop in laminar flow regime. They observed that the Nusselt number increased with induced sonication compared to the cases without sonication, with no significant change in the pressure drop. Esmaeilzadeh *et al.* (2013) worked with γ-Al_2O_3 –water nanofluids under laminar flow regime. Results showed that heat transfer coefficient increased up to 6.8% and 19.1% for volume concentrations of 0.5% and 1%, respectively. Another notable result they outlined was that heat transfer coefficient increases with increasing heat flux.

While convective heat transfer of nanofluids depends on a number of different and interactions based on many studies in the literature, there is no consensus among the reported results (Wang and Mujumdar, 2007; Daungthongsuk and Wongwises 2007) Such discrepancy can be attributed to many factors including; differences in nanoparticles'

shape and size, preparation methods of nanofluids under different conditions. Nanofluids containing even the very same nanoparticles have resulted in different characteristics in terms of thermal behavior. Therefore, there is a need for more experimental investigations in regards to convection heat transfer of nanofluids including different materials and nanoparticles.

1.3. Objective

Considering the fact that hBN containing nanofluids are promising candidates for thermal engineering applications due to their dielectric nature, high in-plane thermal conductivity and graphite/graphen-like structure, there is a need for more detailed studies regarding BN nanofluids. Therefore, one of the objectives of this study is to present a detailed methodology for two step based production of hBN containing, stable nanofluids with 3 different base fluids; water, EG and 50%-50% by volume water-EG mixture. Considering the existing literature, although there are some studies considering production of BN containing nanofluids, there is a certain need for information regarding a detailed 2 step preparation route for hBN nanofluids with different base fluid types and their interactive surfactant amount for stability. Another objective of this study is to contribute to the existing literature regarding BN nanofluids, with a newly introduced thermal stability metric with temporal thermal conductivity characterization. In addition to these, this study aims to examine and outline thermal and rheological characteristics of well dispersed hBN-DI water, EG and mixture of water-EG (50% by volume) nanofluids at different particle concentrations all together and by doing so, it is also aimed to observe the physical significance and effect of hBN nanoparticles dispersed in different base fluids in order to understand the underlying heat transfer enhancement mechanisms. Other than the characterization of thermophysical properties, in order to completely identify the heat transfer behavior of hBN containing nanofluids, convective heat transfer characteristic should be investigated. While there are many studies investigating the convection heat transfer of metal oxide, graphene and CNT containing nanofluids (Wang and Mujumdar, 2007; Daungthongsuk and Wongwises 2007; Gupta *et al.*, 2014), there is no prior study in the literature for hBN nanofluids' forced convection heat transfer behavior. Therefore, there is a certain need for studies investigating the convective heat transfer behavior for hBN nanofluids. For that reason another key aim of this study is to focus on laminar

forced convection of hBN-water nanofluids in a circular copper pipe and identify the change in heat transfer coefficient with respect to the base fluid in order to address this need. As the study is carried out experimentally, a setup is built and validated first, and the forced convective heat transfer behavior of hBN-water nanofluids is then identified and reported for laminar flow.

2. METHODOLOGY

2.1. Experimental Procedure

2.1.1. Nanofluid Preparation and Stability Investigation

Two step method is used in this study for preparation of nanofluids. 70 nm sized hBN nanoparticles, with 99.5% purity (purchased from MK Impex Corp.) are used in the sample preparation procedure. Considering the hydrophobic nature of hBN in polar liquids (ie., DI water, EG), sodium dodecyl sulphate (SDS) and poly vinyl pyrrolidone (PVP K30) are employed with different weight fractions, as surfactants. The morphology of dry nanoparticles are characterized by ESEM imaging (Philips XL30 ESEM-FEG/EDAX) prior to preparation of hBN nanofluids, and a sizing comparison between manufacturer's data and the observed agglomerations that may be formed due to transportation and storage conditions is carried out.

Desired amount of surfactant material is first weighed on a precision balance (Kern PFB, ±10 mg) and then introduced into the base fluid using a mechanical homogenizer (Heidolph, RZR 2021). The optimum weight fraction of surfactant material is determined by an experimental parametric study that targets minimizing the surfactant dependent viscosity increase while achieving long term stability. After obtaining a homogenous surfactant-base fluid solution, desired amount of nanoparticles for different particle volume concentrations varying between 0.03-3%, are weighed and added to the surfactant containing base fluid solutions. The volume concentration of the added nanoparticles is calculated using the measured weight of the dry particles and the hBN density supplied by the manufacturer (2.23 g/cm^3). Nanoparticle containing mixture is first stirred by a mechanical homogenizer for ~30 minutes at ~1500 rpm. Following that, the suspension is placed into ultrasonicator (Hielscher UP400S with sonotrode H22), applying ~140-170 W power. Sonicated nanofluid sample is placed into a temperature controlled water bath (Polyscience 9106A12E) with circulating water temperature set to 12^oC in order to prevent overheating and evaporation. The optimal sonication time for different nanofluids is

determined by a parametric study and it varies from 1 to 3 hours. Details of determination of optimal sonication time are presented by Kurt *et al.* (2013).

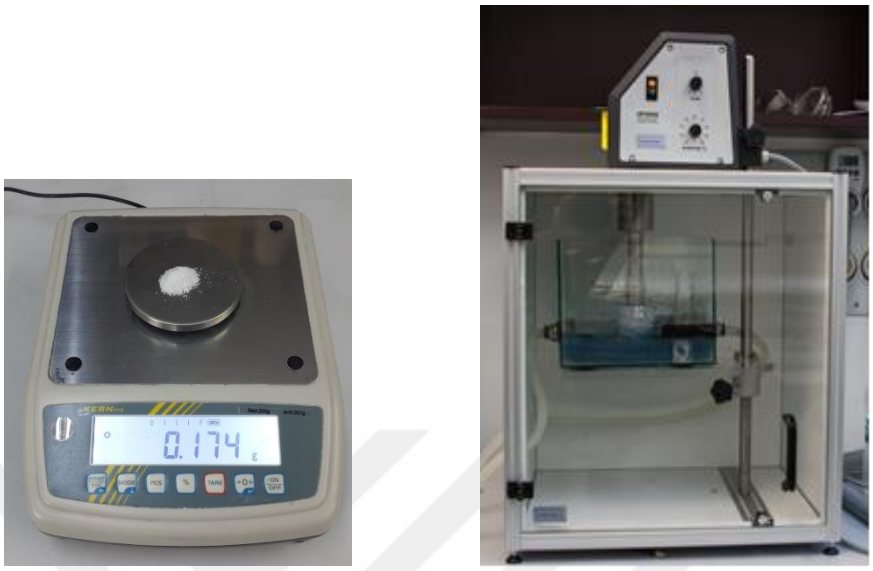

(a) (b)

Figure 2.1. (a) Precision Scale and (b) Ultrasonicator

Following the completion of sonication, agglomerations and particle size distributions in nanofluids are first investigated quantitatively with dynamic light scattering (DLS) method (90 Plus Brookhaven Particle Size and Zeta Potential Analyzer). The measured samples are diluted to 0.01% vol. due to strong opacity of the hBN nanofluids. The diluted sample material is first placed in a standard optical cuvettes and then exposed to incoming laser light with 90^{o} scattering angle. The scattered light intensity will vary due to random motion of the nanoparticles. The device collects the fluctuating signal and uses the data with digital autocorrelator to efficiently calculate particle's diffusion coefficient which is later on used to calculate equivalent spherical particle size by using Stokes-Einstein equation. Although carrying out DLS measurements using diluted samples is arguable, DLS measurements are expected to provide an accurate representation of nanoparticle size distribution, as the dilution process is completed only by utilizing short term mechanical mixing (15 minutes) so that the morphology and the state of agglomerations are not affected.

Another method for investigating the stability of the prepared nanofluids is employed with Zeta Potential measurements (90 Plus Brookhaven Particle Size and Zeta

Potential Analyzer). Again, the measured samples are diluted to 0.01% vol. due to strong opacity of the prepared nanofluids. The zeta potential measurement device utilizes electrophoretic laser light scattering in reference beam mode with realtime. Zeta potential measurements are always done using the 15° detection angle to minimize diffusion broadening. The measurements are performed by using a probe to create electric field within a standard cuvette. This electric field enables nanoparticles to accelerate between two sides and by using laser-doppler anemometry the velocity of these particles is determined. As a result, zeta potential value of nanoparticles within the liquid medium is calculated by relating the velocity of nanoparticles and electrical conductance of the liquid medium to zeta potential. Particle size and zeta potential measurements of nanofluids are only conducted for water based hBN nanofluids since, relatively higher viscosity of the EG and EG-water mixture based hBN nanofluids hinders nanoparticles' accelerated motion between the plates of the measurement device's probe, which results in insufficient amount of sensitivity required for the measurements. Uncertainty range for Zeta Potential measurements are specified as ±0.48-0.71. Particle size and zeta potential measurements are both conducted at 25^{o}C. In order to define the characteristics for a stable colloidal suspension, it should be stated that a suspension with zeta potential (absolute value) above 30 mV are physically stable and below 20mV suspension can be called as with limited stability. Above 50 mV colloidal suspensions exhibit excellent stability and below 5 mV suspensions demonstrate pronounced aggregations (Lee *et al.*, 2008).

Besides the quantitative approaches, qualitative approaches are utilized. The agglomerations of nanoparticles within the nanofluids are observed with a scanning transmission electron microscope (STEM) (Philips XL30 ESEM-FEG/EDAX). The imaging process is completed with air dried nanofluid droplets. The droplets from the prepared nanofluid samples are placed on the copper grids and air dried prior to imaging. Although STEM method provides a colloidal characterization and an insight on morphological dispersion quality of the dried nanofluids, drying process itself may also cause incipient agglomerations overall. Therefore, DLS measurements and STEM imaging should be considered together in terms of particle size determination.

2.1.2. Thermal Conductivity Measurements

Thermal conductivity measurements are conducted at 25^{o}C by a thermal conductivity analyser, using transient hot wire method (Decagon KD2 Pro, ±5-10%). The instrument's KS-1 sensor with 60 mm long, 1.3 mm diameter probe is completely immersed into the measured sample. Low power mode, causing a maximum of 0.5^{o}C temperature increase, is used to diminish errors associated with induced fluid convection. All effects that might lead to convection within the measurement environment are minimized during the experiments, such as; excessive air circulation is prevented by closing the windows and air conditioner during the measurement intervals. While temperature control of the measured sample is attained by placing the sample into a temperature controlled water bath (PolyScience, 9106A12E), during the measurement intervals circulating water bath is turned off to eliminate the induced errors caused by vibration and convection. Experimental test setup can be observed from Figure 2.1.

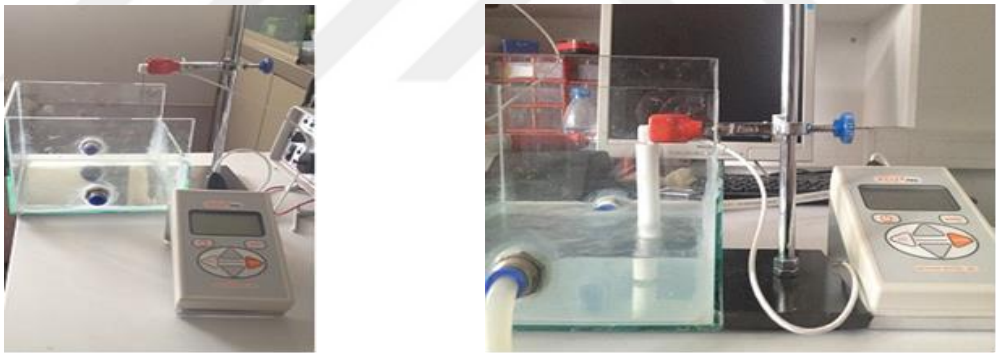

Figure 2.2. Thermal conductivity measurement test setup

2.1.2.1. Reproducibility and Uncertainty. All the measurements are repeated at least 10 times and the mean value of these measurements is reported. The uncertainties of the nanofluid to base fluid thermal conductivity rates presented are estimated based on the uncertainty analysis outlined by Kline and McClintock (1953). The accuracy of the thermal conductivity measurements are tested with DI water, ethylene glycol and KD2 Pro's calibration liquid, glycerol, at the specified temperatures within the range of 20-25^{o}C and the obtained calibration results are validated with corresponding data provided in literature. Validation measurements with DI-water, EG samples and glycerol are within 5% of data provided in literature. The results of thermal conductivity measurements for

nanofluids are presented with their respective uncertainty range and it is found that standard deviation of the thermal conductivity measurements is less than 3% of the mean value. While all presented results represent the mean of consecutive measurements, a dynamic reproducibility study was also carried out to gain a level of trust to the specified production methodology. Seven different samples of 1% hBN-DI water nanofluid are produced following the same recipe, and samples' thermal conductivity and viscosity are measured. It was found that the standard deviation of measured thermal conductivity for these samples was 2.8% of the mean value. Considering that standard deviation of viscosity is even smaller, it can be concluded that measured properties of the produced samples was found to be within the limits of measurement sensitivity. Moreover, all nanofluid samples with different volume concentrations and base fluid types are produced at least 3 times to check the reproducibility. Initial values of thermal conductivity measurements are obtained right after the nanofluid preparation is complete. Temporal investigation of prepared nanofluids' thermal conductivity is conducted to evaluate the long term use of nanofluids for typical applications where nanofluid is subjected to forced flow. For that reason, time dependent thermal conductivity measurements are carried out on a daily basis, and all the nanofluid samples are mechanically stirred for 5 minutes at 500 rpm prior to each temporal thermal conductivity measurement.

2.1.3. Viscosity Measurements

A cone-plate rheometer (Brookfield DV-III Ultra) with temperature sensor is used to investigate the rheological behaviour of nanofluids at 25^{o}C. Standard plates with 0.8^{o} and 3^{o} cone angle (CP40 and CP41) are employed to measure viscosity and shear stress, with respect to shear rate applied. The specified cone plates are connected to the spindle drive and, having a specific gap length between the sample and the cone plate; the measured sample is placed in the sample cup. As the spindle is rotated, viscous drag of the sample is measured by means of deflection of the calibration spring in the rheometer. Temperature control of the measured samples is attained by connecting a temperature controlled water bath (PolyScience, 9106A12E) to the sample cup. The uncertainty of the measurements change with the shear rate and the viscosity range, and the maximum error is 0.1% of the full range of measurable viscosity at the specified shear rate. The calibration of the device is carried out by measuring the DI-water and EG samples'

rheological behavior at 25 ^{o}C, and the results are validated by comparing with the data in literature.

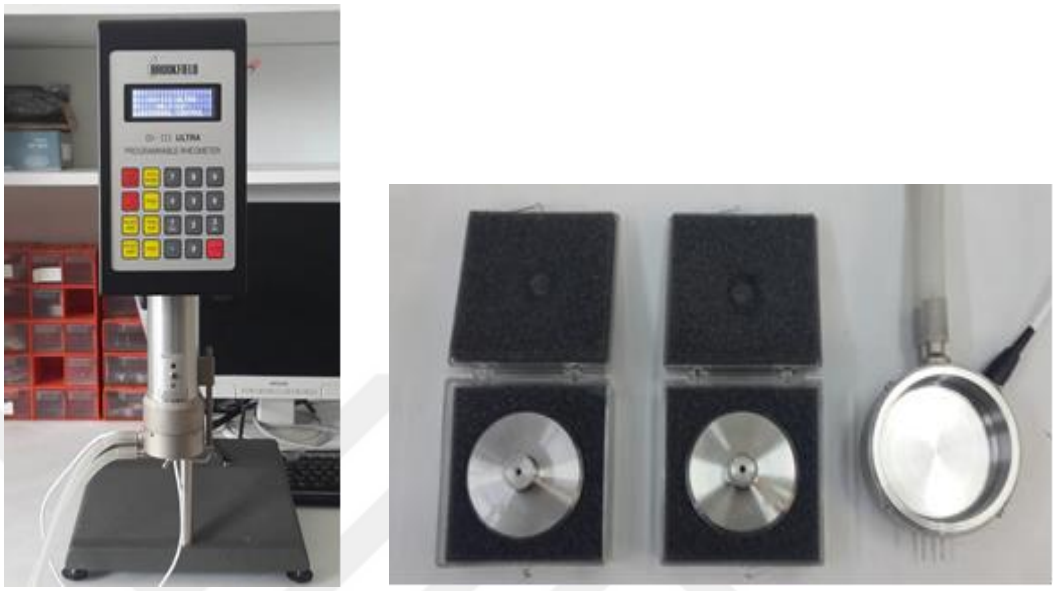

(a) (b)

Figure 2.3. (a) Brookfield DV-III Ultra cone plate rheometer, (b) CP40 and CP41 spindles and sample cup

2.1.4. Convective Heat Transfer Measurements

An experimental test setup is developed and manufactured considering laminar thermally developing flow in a uniformly heated circular copper pipe so that local heat transfer coefficient can be measured. The test setup is first validated by experiments using DI-water. It is then used for testing hBN-water nanofluids with different particle volume concentrations, and flow rates. Thermal conductivity and viscosity of the nanofluids are measured prior to testing their convective behavior. In order to investigate the effects of testing conditions on nanofluid samples, thermophysical properties of hBN nanofluids are also measured right after the conducted laminar flow experiments. It is found that tested samples' properties are in agreement with the prior values, in terms of both stability and thermal conductivity metrics. For that reason it can be stated that, testing procedure does not cause any change or deterioration on the thermophysical properties of tested nanofluids.

2.1.4.1. Experimental System. A schematic of the constructed experimental system for this study is shown in Figure 2.1. The test system is designed and built for identifying forced convective heat transfer coefficient in the horizontally oriented circular copper pipe subjected to uniform heat flux. Experimental system consists of a test unit where the fluid is heated, a cooling unit, reservoir, and pump. The test unit is constructed of a horizontal straight copper tube with approximately 2 m length, 6 mm inner and 8 mm outer diameter. The first 0.5 m length of the tube is left unheated so that the flow hydrodynamically develops before it is subjected to uniform heat flux boundary condition.

The heated section of the test unit is first electrically insulated with fiberglass sleevings, then helically coiled bare nichrome heater wire is uniformly wrapped around the copper pipe to provide uniform heat flux along the heated section. The AC powered heater is controlled by a potentiometer and the maximum applied power is 450 W. Heater wire is then coated with zinc phosphate based cement layer to provide uniform heating. The coated heater is firmly wrapped with fiber-glass electric insulation tapes. A thick thermal insulation layer is applied to minimize the heat loss to the environment. Details of the construction of heated section is presented in Figure 2.1.

Figure 2.4. Built-up steps for heating section

Six T-type thermocouples (Omega Inc.; σ_T = ±0.5^{o}C) are mounted with thermal epoxy on the test tube wall at dimensionless axial locations *(x/D)* of 18.8, 72.5, 97.5, 140, 183, 251 starting from the beginning of the heated section. Two T-type thermocouples are submerged into the flow to measure the fluid temperature at the inlet and exit of the heating unit. The data is recorded using a data acquisition system (Agilent 34970A). The

temperature values of tube wall surface and fluid are recorded for a duration, after the system reaches steady state, and time averaged values over this duration are considered.

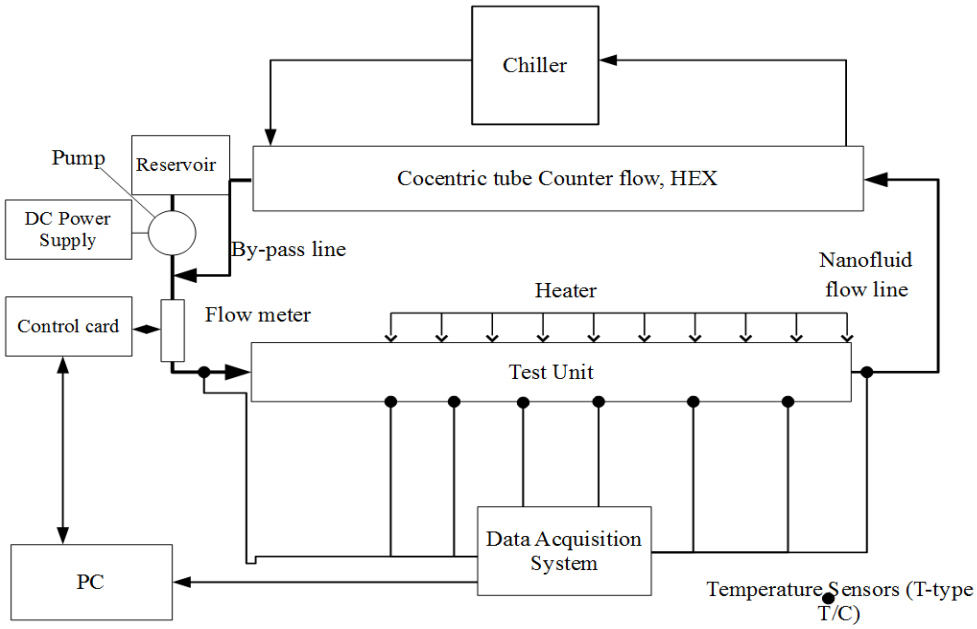

Figure 2.5. Schematic of experimental system

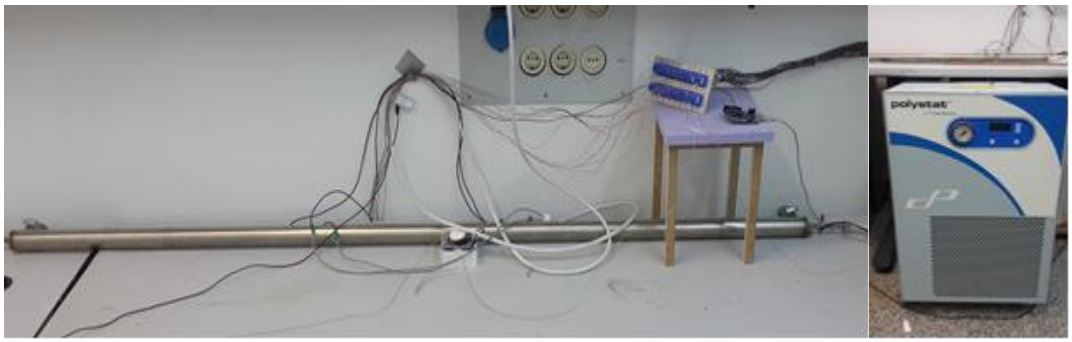

Figure 2.6. Counter flow cocentric tube heat exchanger and chiller

In order to achieve a steady state, heated fluid flows through a counter flow cocentric tube heat exchanger, connected to a chiller (Polysat 12920) before it returns to the reservoir. The flow is provided by a centrifugal pump (Iwaki RD-20) that is linked to a reservoir placed right after the cooling unit. The flow rate is measured by and it is adjusted using a valve.

2.1.4.2. Data Analysis. The specific heat and density of the nanofluids are calculated based on simple mixture rule that can be presented as:

$$\rho_{nf} = (1-\varphi)\rho_{bf} + \varphi\rho_{np} \tag{2.1}$$

$$c_{p,nf} = \frac{(1-\varphi)\rho_{bf}c_{p,bf} + \varphi\rho_{p}c_{p,p}}{\rho_{nf}} \tag{2.2}$$

where φ is the particle volume concentration of the suspension, subscripts *p, bf* and *nf* indicate the particle, base fluid and nanofluid properties, respectively. The properties for dry hBN nanoparticles are adopted from NIST.

The calculation of the local heat transfer coefficient based on Newton's law of cooling can be summarized as follows:

$$h_x = \frac{q_s''}{T_s(x) - T_m(x)} \tag{2.3}$$

where, q_s", T_s (x), T_m (x) represent the applied heat flux, wall temperature and mean temperature of the fluid at a given axial position, *x*, in the test section, respectively. The thermocouples are mounted on the outer surface of the tube, and the difference between inner and outer wall surface temperatures of the copper test tube is estimated approximately 0.1^{o}C for the applied heat fluxes. The mean temperature of the fluid at any axial location along the test section can be defined as:

$$T_m(x) = T_{m,i} + \frac{q_s'' \pi D_h x}{\dot{m} c_p} \tag{2.4}$$

where $T_{m,i}$ demonstrates mean temperature of the fluid at the inlet. Combining Eqs. (2.3) and (2.4) local heat transfer coefficient can be redefined as;

$$h_x = \frac{q_s''}{T_s(x) - T_{m,i} - \frac{q_s'' \pi D_h x}{\dot{m} c_p}} \tag{2.5}$$

The local Nusselt number is defined as;

$$Nu_x = \frac{h_x D_h}{k} \tag{2.6}$$

2.1.4.3. Experimental Uncertainties. Single sample measurement uncertainty, explained by Kline and McClintock (1953), is adopted to calculate the uncertainty of the experimental heat transfer coefficient and Nusselt number.

$$\sigma_h(x) = \left[\left(\frac{\partial h_x}{\partial \dot{m}} \sigma_{\dot{m}} \right)^2 + \left(\frac{\partial h_x}{\partial T_s} \sigma_T \right)^2 + \left(\frac{\partial h_x}{\partial T_m} \sigma_T \right)^2 + \left(\frac{\partial h_x}{\partial q''} \sigma_{q''} \right)^2 \right]^{1/2} \tag{2.7}$$

$$\sigma_{Nu}(x) = \left[\left(\frac{\partial Nu_x}{\partial \dot{m}} \sigma_{\dot{m}} \right)^2 + \left(\frac{\partial Nu_x}{\partial T_s} \sigma_T \right)^2 + \left(\frac{\partial Nu_x}{\partial T_m} \sigma_T \right)^2 + \left(\frac{\partial Nu_x}{\partial q''} \sigma_{q''} \right)^2 + \left(\frac{\partial Nu_x}{\partial k} \sigma_k \right)^2 \right]^{1/2} \tag{2.8}$$

As can be seen from the Eqs. (2.7) and (2.8), the uncertainties of measured heat transfer coefficient and Nusselt number are dependent upon the uncertainties of flow rate, temperature, heat flux and thermal conductivity measurements. While uncertainties in regards to flow rate, temperature and thermal conductivity measurements are presented in the previous sections, the uncertainty with regards to the applied heat flux must be predicted in a similar way. The applied heat flux to the system can be defined by

$$q_s'' = \frac{\dot{m} c_p}{\pi D_h L}\left(T_{m,o} - T_{m,i}\right) \tag{2.9}$$

and the corresponding uncertainty can be defined as;

$$\sigma_{q_s''} = \left[\left(\frac{\partial q_s''}{\partial \dot{m}}\sigma_{\dot{m}}\right)^2 + \left(\frac{\partial q_s''}{\partial \dot{T}_{m,o}}\sigma_T\right)^2 + \left(\frac{\partial q_s''}{\partial \dot{T}_{m,i}}\sigma_T\right)^2\right]^{1/2} \tag{2.10}$$

The study considers thermal entry length of laminar forced convection in a circular test unit subject to uniform heat flux. For these conditions a correlation proposed by Churchill and Ozoe (1973) can be used for defining the Nusselt number that is given as:

$$\frac{Nu_x + 1}{5.364} = \left[1 + \left(\frac{220}{\pi} x^+\right)^{-10/9}\right]^{3/10} \tag{2.11}$$

where,

$$x^+ = \frac{x}{D_h Re_D Pr} \tag{2.12}$$

The measurement uncertainty can be predicted considering the Churchill and Ozoe (1973) correlation and presented uncertainty analysis. The relative uncertainty of the measurement setup, $\sigma_h (x)/h_x$ and $\sigma_{Nu} (x)/Nu_x$, is presented in Figure 2.2. It can be observed that resulting uncertainty in Nusselt number for the system is bounded by 7%, whereas uncertainty of the heat transfer coefficient is bounded by approximately 5%.

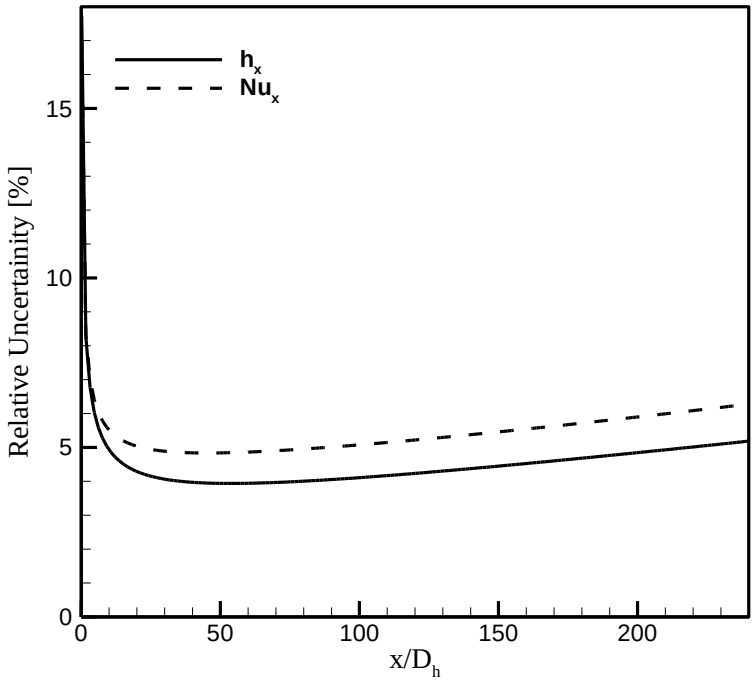

Figure 2.7. Calculated relative uncertainty along with test section

3. RESULTS AND DISCUSSION

3.1. Dry Nanoparticle Characterization

Scanning Electron Microscope characterization is carried out for dry hBN nanoparticles in order to investigate preliminary form of dry particles' agglomeration state, prior to nanofluid preparation. As can be seen in Figure 3.1., hBN's primary particles have a platelet like shape with a mean diameter of 60-80 nm, but aggregates are formed with an average size at least 4 times larger than the manufacturer's specifications. Therefore, processes such as ultrasonication and surfactant addition must be employed in 2 step method to reduce the agglomerate sizes to obtain well dispersed nanofluid solutions.

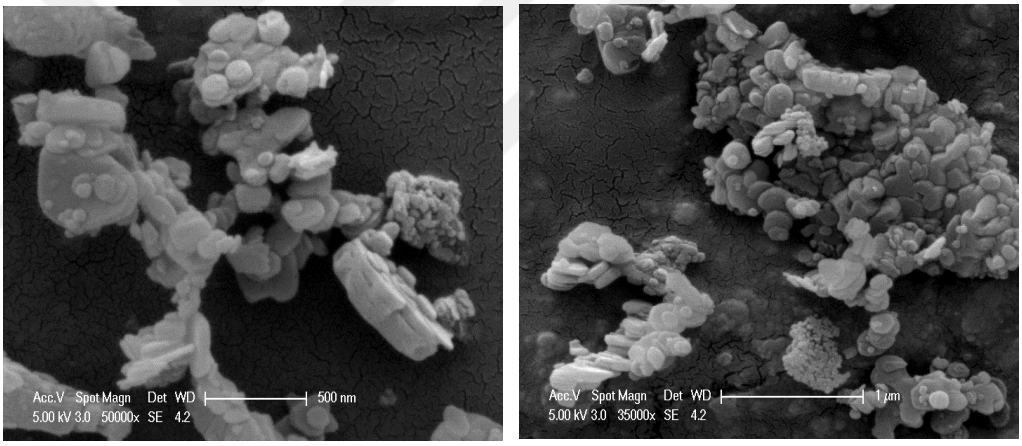

Figure 3.1. ESEM image showing aggregate state of dry hBN nanoparticles

3.2. Optimizing Surfactant Additives

Surfactant free nanofluids are prepared first, using only mechanical mixing and ultrasonication. It was found that sedimentation occurs after several hours for all base fluids when no dispersing agents are used. Based on these results, it is decided to use surfactant materials as a part of 2 step method. Surfactant or any other dispersant agent use is a commonly employed method for increasing stability of nanofluids. Although this is an easy to implement procedure, using surfactant materials might also suppress the enhancement of thermal performance by foaming, increasing the viscosity of the base fluid, or by increasing the thermal resistance between nanoparticles and base fluids (Xuan

et al., 2013). Therefore, effects of two different surfactant materials, SDS and PVP, on long term stability, base fluid viscosity and thermal conductivity are investigated. Both surfactant materials are added to the 3 different base fluids with different weight fractions ranging from 0.003% to 0.5%. After dispersing these reagents, changes in both viscosity and the thermal conductivity of the base fluid solutions are investigated. It was found that surfactant additives' effect on sole base fluid thermal conductivity is within the negligible range with respect to measurement limits. The incremental change can be observed from Figure 3.2. for the case of viscosity increase, where μ_{bf} and μ_{sf} denotes viscosities of the base fluid and the surfactant containing base fluid, respectively. Up to 0.1% by weight, both surfactants' effect on all the base fluids can be considered as negligible (<3%). However, for weight fractions exceeding 0.1%, viscosity increase becomes significant especially for EG and EG/water (50% by volume) base fluids. It can also be observed in Figure 3.2 that addition of SDS to water leads to the smallest viscosity change compared to other base fluids containing PVP. Zhou *et al.* (2012) investigated the effect of SDS and PVP at different weight fractions on viscosity and they stated that viscosity of PVP containing solutions rises quicker than SDS containing ones even at low concentrations that is in agreement with results presented in Figure 3.2.

Following the identification of the effect of surfactant additives on viscosity and thermal conductivity of base fluid, stability inspection of hBN nanofluids is conducted. hBN nanofluids are prepared by incrementally increasing the surfactant concentration in order to minimize the viscosity increase of nanofluids while sedimentation levels of nanofluids are inspected. If sedimentation is observed within 12 hours, amount of surfactant added is increased. It was found that although 0.1% SDS by weight increases the stability of the water based hBN nanofluids, it does not positively affect the dispersion quality of EG and EG/water based nanofluids. Even up to 0.5% by weight, SDS addition did not improve stability for EG and EG/water based nanofluids. Therefore, effect of SDS on EG and EG/water base fluids' viscosity is not reported. It was also observed that SDS addition causes foaming. Therefore, PVP is considered as the only surfactant material for the further stages of this study.

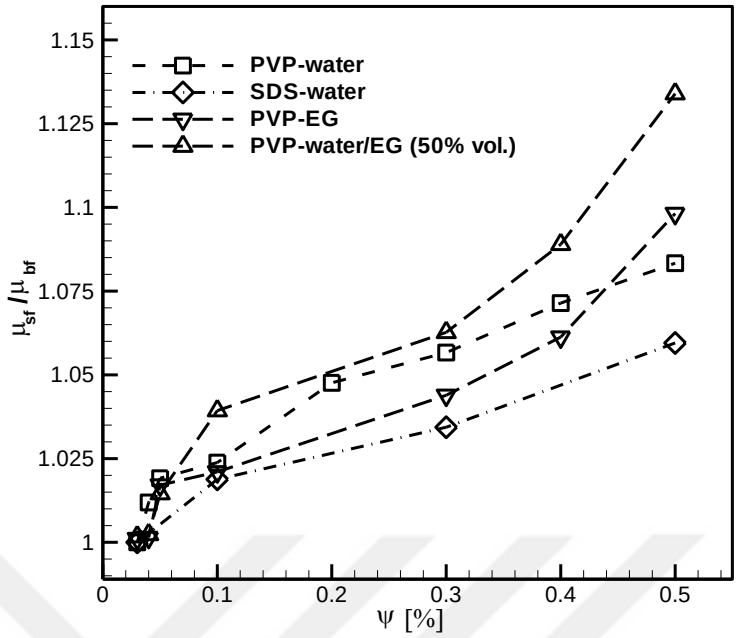

Figure 3.2. Change in the viscosity of surfactant, PVP and SDS, containing base fluids

After stability inspection of nanofluids with different weight concentrations of SDS and PVP, it was found that ideal surfactant amount of water based nanofluids is 0.05% by weight for nanofluids containing less than 1% particle volume concentration and 0.1% by weight for nanofluids with 1-3% particle volume concentration for both SDS and PVP. For EG based hBN nanofluids, ideal PVP amount is determined to be 0.1% by weight for nanofluids with up to 3% particle volume concentration, and for 3% of hBN; 0.3% by weight of PVP. For EG/water (50% by volume) based nanofluids, optimum amount of PVP addition is determined to be 0.1% by weight for particle volume concentrations less than 3% and, 0.35% by weight, for particle volume concentration of 3%. Experimental details of all the presented nanofluids with respect to preparation procedure are summarized in Table 3.1.

Table 3.1. Detailed preparation procedure of hBN nanofluids

Nanofluid	φ [% by vol.]	Ultrasonication duration (hr)	Surfactant	Surfactant [% by weight]
hBN-water	1,2,3	1-1.5	SDS	0.1
hBN-water	0.03-0.5	1	PVP	0.05
	1, 2, 3	1-1.5		0.1
hBN-EG	0.5,1,2	1-1.5	PVP	0.1
	3	1.5		0.3
hBN-water-EG	0.5,1,2	1-1.5	PVP	0.1
	3	1.5		0.25

3.3. Stability Investigation

Quantitative evaluation of the preparation procedure and optimal surfactant amounts is carried out by inspecting temporal change in Zeta Potential and thermal conductivity ratio. Temporal thermal conductivity measurements can be considered as a good quantitative metric for determining the stability level of nanofluids (Wang *et al.*, 2012; Yu *et al.* 2010; Timofeeva *et al.*, 2007; Kole and Day, 2013; Yu *et al.*, 2009). In order to investigate the relation between time dependent thermal conductivity change and level of stability, time dependent Zeta Potential and thermal conductivity measurements are conducted for 0.1% hBN-water nanofluid. Zeta Potential of 0.1% hBN nanofluids indicates acceptable stability level up to 5 days as can be seen in Figure 3.3. Similar trend can also be seen for temporal thermal conductivity change. Although change in the thermal conductivity ratio is not as significant, disputable thermal conductivity decrease can be observed after several days. It should be noted here that Zeta Potential measurements are carried out with diluted samples of hBN-water nanofluids to 0.01% volume concentration due to opacity of the 0.1% hBN nanofluid. Here, the nanofluid samples are rehomogenized using a mechanical mixer before each thermal conductivity measurement in order to prevent layering. The effect of mechanical mixing can be considered similar to that of nanofluid running through turbo-machinery used for many engineering applications with forced flow. Considering the similar pattern between

temporal changes in thermal conductivity and Zeta Potential results in Figure 3.3., it can be concluded that temporal thermal conductivity measurements can be used to identify the stability state of nanofluids. Moreover, in this study zeta potential measurements of nanofluids could only be conducted for water based hBN nanofluids, due to relatively higher viscosity of the EG and EG-water mixture based nanofluids. The higher viscosity base fluid hinders nanoparticles' motion between the plates of the measurement probe, which limits the sensitivity of the measurements. Therefore, time dependent stability inspections of hBN nanofluids in this study are presented in terms of thermal conductivity.

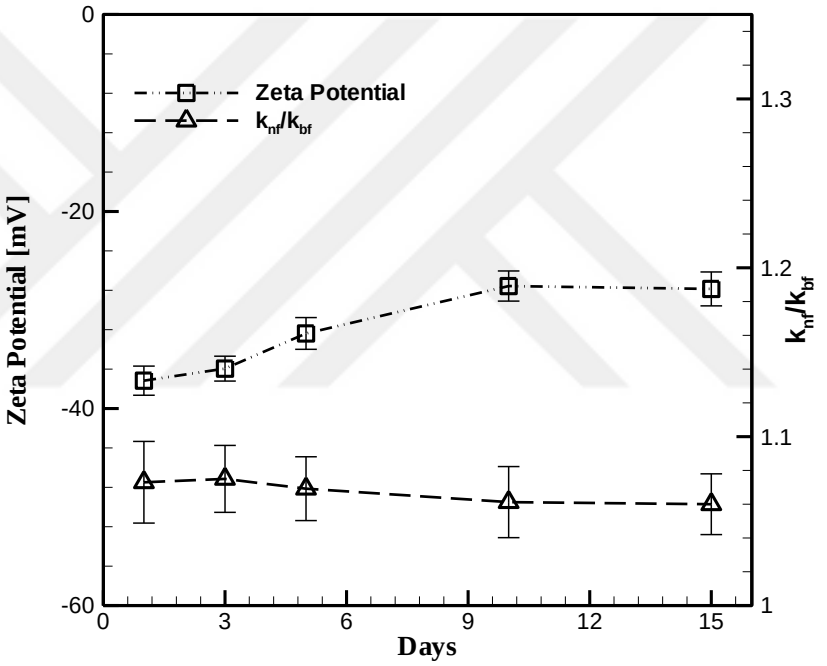

Figure 3.3. Temporal change in the Zeta potential and thermal conductivity ratio of 0.1% hBN-water nanofluids with respect to elapsed days

Considering the correlation between stability and thermal conductivity enhancement, temporal change in the thermal conductivity of samples with volume concentrations of 1, 2 and 3% for water based, and 1% volume concentration for EG and EG-water mixture based nanofluids are investigated and presented in Figure 3.4. It can be observed in Figure 3.4. that 1% nanofluids exhibit long term stability with a maximum decrease of 3% in thermal conductivity within 15 days. Such observation leads to a conclusion that 1% volume concentrated nanofluids exhibit high level of stability and have

long term shelf life. Relatively small changes for thermal conductivity ratio is within the measurement uncertainty. For higher particle volume concentrations such as 3%, a sharp decrease in thermal conductivity within several days can be seen for water-hBN nanofluids, and following that thermal conductivity ratio remains unchanged. Considering the fact that the weight fraction of PVP is 0.1% for all nanofluids presented in Figure 3.4, the amount of surfactant used can be increased to obtain higher level stability for particle volume concentrations greater than 2%. While evaluating the amount of surfactants, its effect on thermal conductivity and viscosity should also be considered. Excessive amounts of surfactants may cause increase in base fluid viscosity and also super-saturation of surfactant materials can deteriorate heat transfer performance by creating a thermal resistance layer on nanoparticles or by limiting their movement. Several effects should be taken into consideration while determining the required amount for the specific applications, such as oversaturation of surfactant material and required pumping power.

One of the major outcomes that can be drawn from temporal thermal conductivity measurements is highly related to the effect of mechanical mixing. Reminding that all the measurements are conducted right after mechanical mixing, the stability of the prescribed nanofluids can be well preserved with mechanical mixing. Even though partial sedimentation and coagulation might occur with the nanofluid by causing layering, with the application of mechanical mixing homogeneity of these colloidal suspensions can be reached via short time of mixing. Figure 3.5. demonstrates the change in the homogeneity of 1% hBN-EG and 1%hBN-water nanofluid after 3 weeks to preparation.

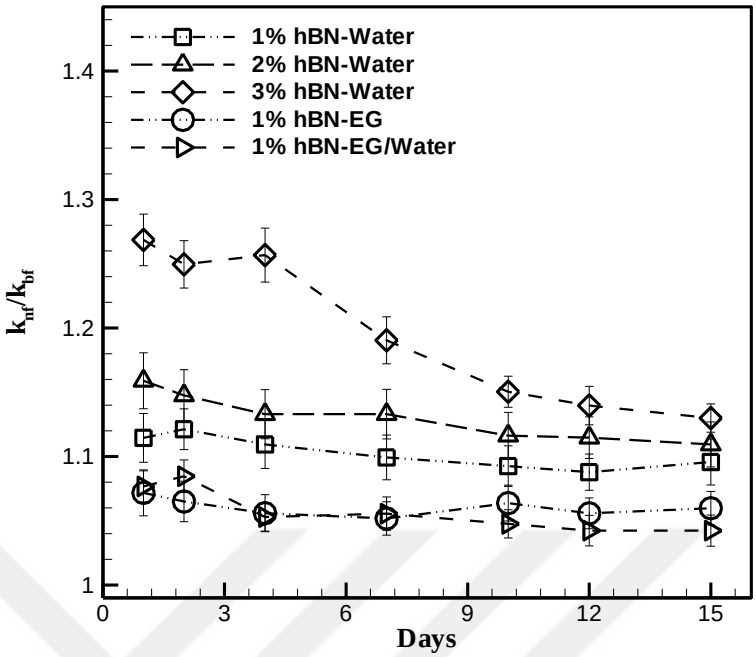

Figure 3.4. Temporal thermal conductivity measurements of hBN nanofluids

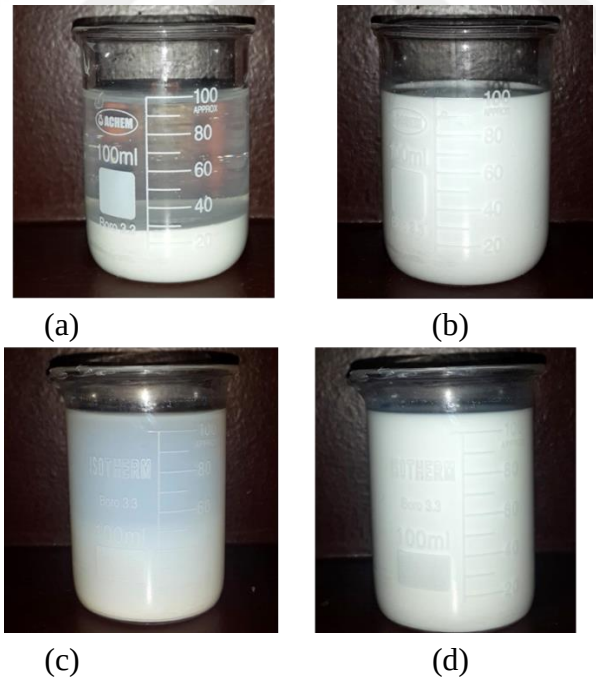

Figure 3.5. Temporal change in the homogeneity of nanofluids (a) After 3 weeks 1% hBN-EG (b) Right after mech. mixing (c) After 3 weeks 1% hBN-water (b) Right after mech. mixing

Nanoparticle aggregates are inspected with DLS measurements, and the results are presented in Figure 3.6. DLS measurements are first conducted with water based nanofluids for 3 different particle volume concentrations, 0.1, 0.5 and 2%, to evaluate the effect of particle loading on average particle size distribution. Particle size distribution by number shows a bimodal distribution for all particle volume concentrations with distribution peaks close to the size of primary nanoparticles. It can be seen that although, there still exists cluster formations within the medium, average particle size of aggregates are reduced to 40-60 nm range, meaning that large and densely populated aggregates observed in dry nanoparticles are broken with ultrasonication process and surfactant addition is an effective method for all particle volume concentrations for water based nanofluids.

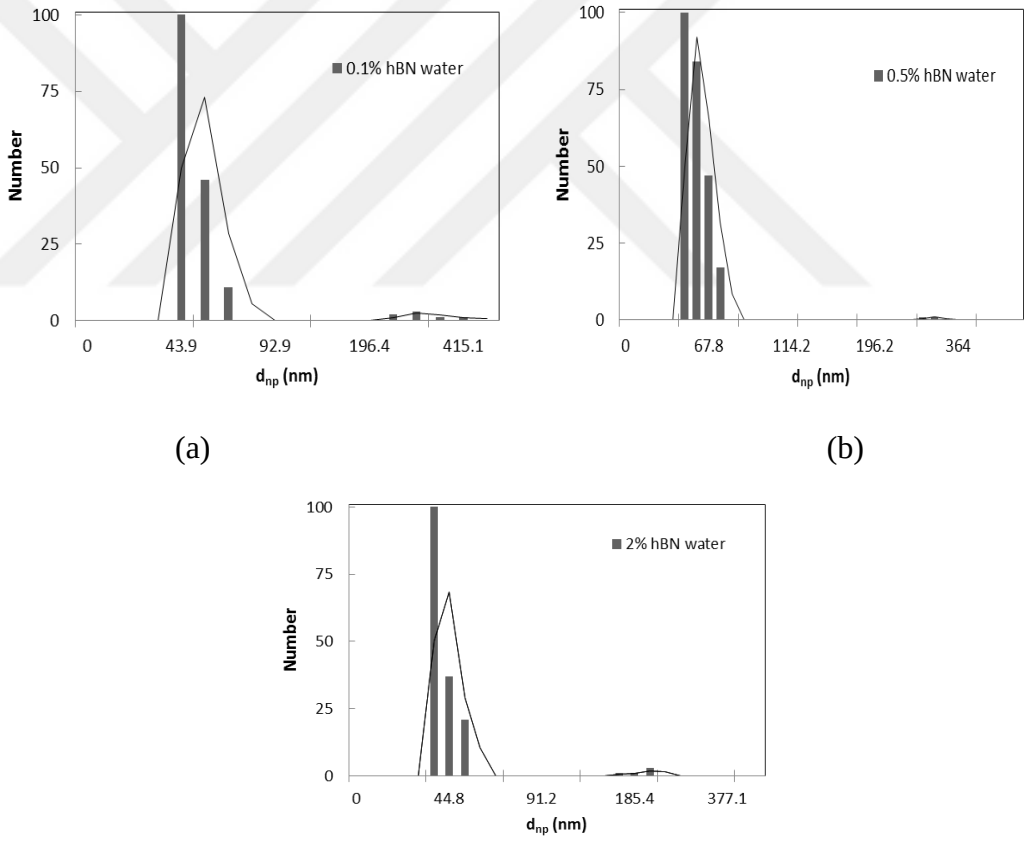

Figure 3.6. Particle size distribution of a) 0.1% hBN-water, b) 0.5% hBN-water, c) 2% hBN-water

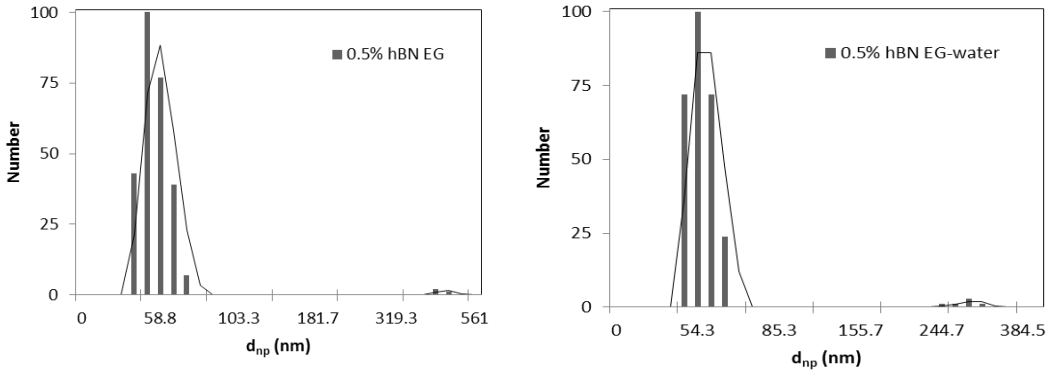

(a) (b)

Figure 3.7. Particle size distribution of a) 0.5% hBN-EG, b) 0.5% hBN-EG-water

. Similarly, DLS measurements are also conducted for EG and EG-water mixture based nanofluids for 0.5% volume concentration and the results can be observed from Figure 3.7. Similar particle distribution can also be observed for these nanofluids with bimodal distribution peaks at approximate sizes of primary particles' mean diameter. With the applied preparation recipe, majority of the agglomerations are broken into smaller sized particles approximately in the range of 40-70 nm, indicating that particle size distribution is also independent of base fluid type as well as the volume concentration.

Morphological characterization of dispersed nanoparticles is also conducted with STEM imaging. Agglomeration state and alignment of particles can be observed in Figure 3.8. for water based nanofluids, and in Figure 3.9. for EG and EG/water based nanofluids. For water based nanofluids, it can be observed that most of the large clusters formed by densely populated primary particles are broken down, and hBN nanoparticles align in a loose chain like structure that appears as an interconnecting network acting as a heat conducting path. Moreover, poly-dispersed stage of particle distribution can also be observed as some of the nanoparticles are forming local clusters as percolating structures, whereas some of them are in the form of dynamic free particles. Li *et al.* (2001) observed similar morphological structure and claimed that BN nanoparticles form a chain structure contributing to a large thermal conductivity increase for their BN-EG nanofluids with low particle volume concentrations (0.025%). Similar observations are mostly encountered in studies with graphene oxide (GO), CNT and Fe_3O_4, CuO containing nanofluids (Gupta *et al.*, 2011; Yu *et al.*, 2009; Karthikeyan *et al.*, 2007; Murshed *et al.*, 2008). However, such

an interconnecting network cannot be observed for EG based nanofluids. Particles are almost mono-dispersed within the base fluid and structures similar to those in Figure 3.8 cannot be observed in Figure 3.9(a). For EG/water based nanofluids, which can be seen in Figure 3.9(b), poly-dispersed state can be observed even though it is not as clear as it is for water based nanofluids.

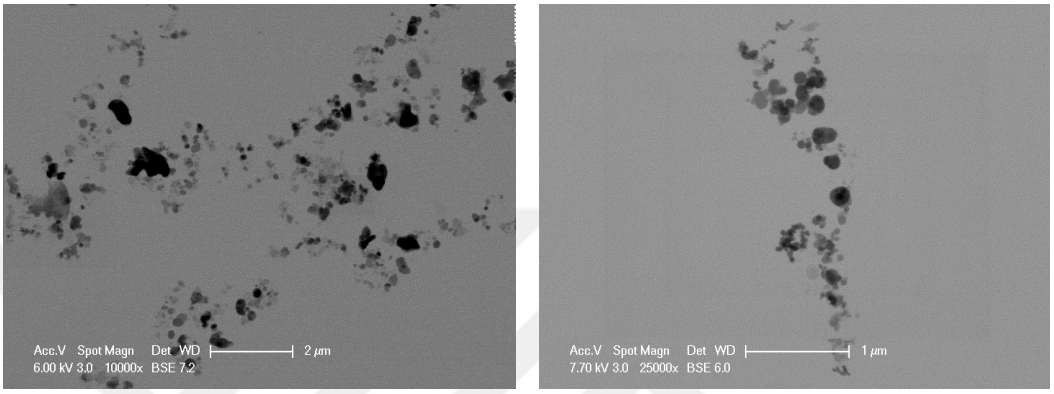

(a) (b)

Figure 3.8. STEM image showing morphology of water-hBN nanofluids with (a) 0.5% and (b) 0.1% particle volume concentration.

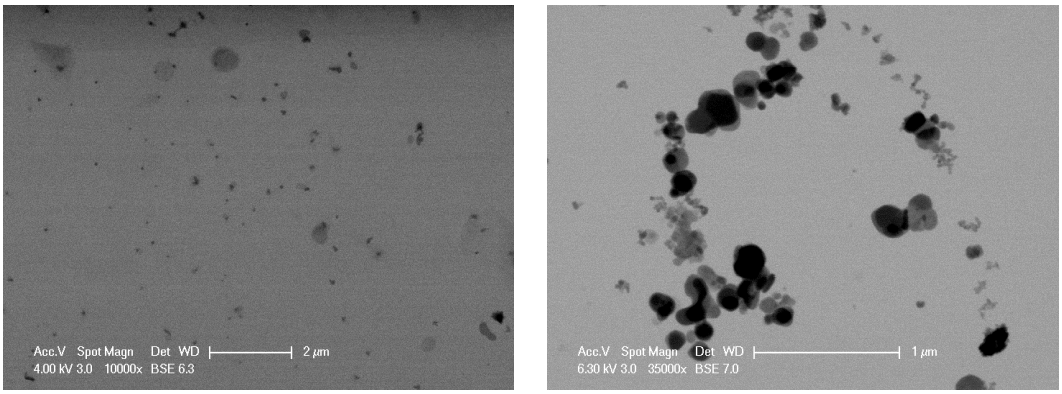

(a) (b)

Figure 3.9. STEM image showing morphology of (a) EG based, (b)EG/water based hBN nanofluids with 0.5% particle volume concentration

3.4. Thermal Conductivity of Nanofluids

Thermal conductivity of water, EG and water/EG mixture based hBN nanofluids with respect to particle volume concentration is investigated next. The hBN nanofluids are prepared using the two step method with production recipe summarized in Table 3.1. The measured change in nanofluid to base fluid thermal conductivity ratio with respect to particle volume concentration is presented in Figure 3.10. A significant increase in thermal conductivity is observed for water-hBN nanofluids with very small particle volume concentrations ($\varphi \leq 0.1\%$). Thermal conductivity increases by ~7% for 0.1% particle volume concentration. Beyond this point, as particle loading is further increased, the rate of increase slows down. For particle volume concentrations higher than 0.5%, the observed enhancement slightly exceeds linear increasing trend, and thermal conductivity increase is 26% for hBN-water nanofluid with 3% particle volume concentration. Considering the pattern in Fig. 3.9, thermal conductivity for hBN–water nanofluids should be considered in 2 segments with different curvatures representing different rates of increase. Therefore, for hBN–water nanofluids with $\varphi \leqslant 0.1\%$ the effective thermal conductivity can be represented as.

$$\frac{k_{nf}}{k_{bf}} = 11{,}157\varphi^2 + 62.29\varphi + 1 \tag{3.1}$$

and for $\varphi > 0.1\%$

$$\frac{k_{nf}}{k_{bf}} = 172\varphi^2 - 0.03\varphi + 1.1008 \tag{3.2}$$

While it is hard to comment on the governing mechanisms explaining the observed trends based on Figure 3.10., using micrographs of hBN-water nanofluids for 3 different volume concentrations (0.1, 0.5, 2 %) as shown in Figure 3.11. can be helpful. The local cluster formations as loosely packed chains can be observed in Figure 3.11(a) for 0.1% particle volume concentration. The sudden increase in thermal conductivity at low particle concentrations can be explained by initialization of poly-dispersed state, where dynamic free particles and local cluster formations coexist, and these local cluster formations create

paths of low thermal resistance within the suspension. Effective volume of a cluster is much larger than the actual volume of the nanoparticles in this state, leading to formation of highly conductive heat transfer paths within the medium even at low particle concentrations. As particle loading increases, the packing fraction, which is the ratio of the individual nanoparticles forming clusters to the cluster effective volume, increases leading to a denser, more particle populated network as shown in Figure 3.11(b). Although this leads to a further increase in thermal conductivity, it is not as effective as introducing new thermal paths or spreading them to a larger volume. Therefore, the thermal conductivity increase rate slows down. Similar morphological state can also be observed in Figure 3.11(c). for 2% hBN-water, where local clusters are formed with a larger particle population leading to denser structures and slower effective thermal conductivity increase rate.

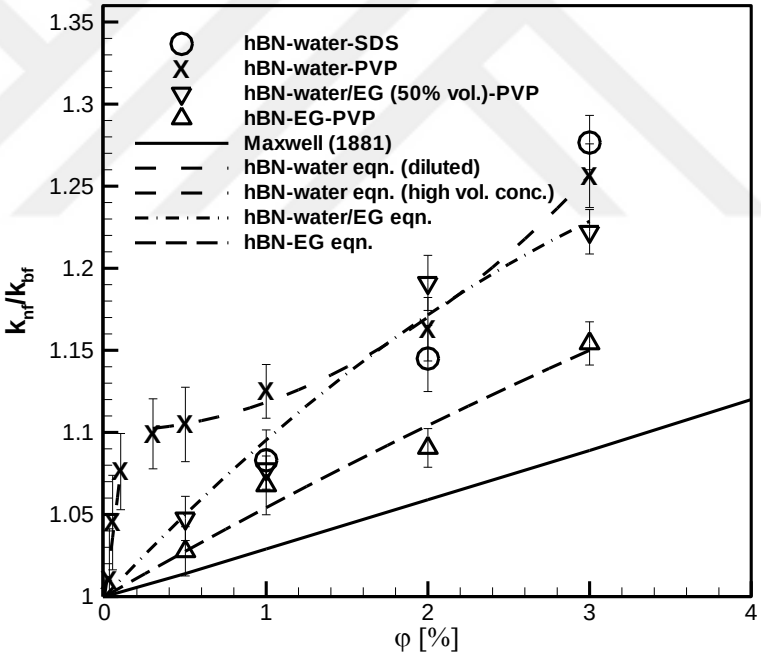

Figure 3.10. Change in nanofluid to base fluid thermal conductivity ratio of hBN nanofluids.

Keblinski *et al.* (2002) also explains such distinctive thermal conductivity increase trend with particles not in close physical contact, claiming that, such liquid mediated clusters are actually forming an interconnecting network with very low packing fraction leading to a larger effective volume of a local cluster. Therefore, it can be concluded that

percolation is the major enhancement mechanism and creating new clusters is more effective in enhancing thermal transfer than increasing the packing fraction of existing clusters. There are similar thermal conductivity trends observed in the literature and the mechanisms outlined above are in agreement with those observed in literature, such as Keblinski *et al.* (2001), Wang *et al.* (2012), and Zhu *et al.* (2006).

Besides the morphology of nanoparticles, crystal structure of hBN and its anisotropic heat transfer characteristics due to high in plane thermal conductivity should also be considered. Platelet shaped nanoparticles appears to be aligned in the direction conductivity is higher due to higher surface attraction forces, while forming the local clustering structures that further supports the percolation dominated enhancement. Moreover, creating more branched networks of particles appears to be more effective than increasing the packing fraction of existing clusters. While these observations are aligned with the presented data and micrographs, these effects must be investigated through multi-scale modeling of the system, combining molecular to meso-scale modeling approaches.

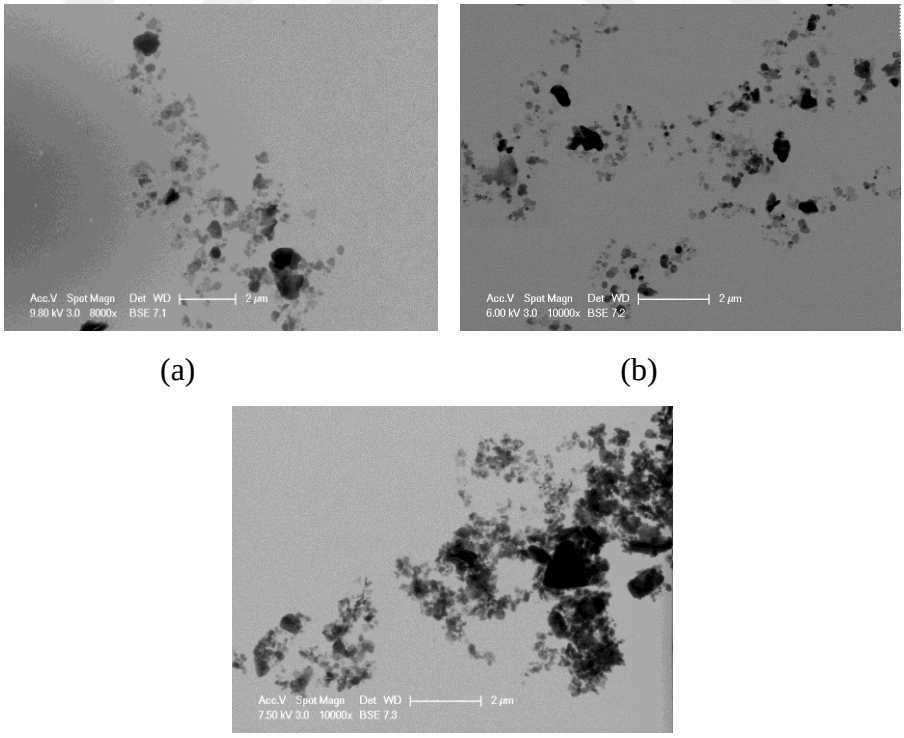

(a) (b)

(c)

Figure 3.11. STEM images of water-hBN nanofluids with (a) 0.1% , (b) 0.5%, (c) 2% particle volume concentration.

While there is a distinctive pattern for water based nanofluids, including noticeable enhancement at lower volume concentrations, EG and EG/water based nanofluids are not demonstrating such behavior. EG/water mixture based nanofluids are also tested for thermal conductivity increase at relatively smaller particle volume concentrations and it is found that such distinctive enhancement is not present. At 0.5% volume concentration, EG/water based nanofluids demonstrate a relatively small thermal conductivity enhancement of ~4.7%. Although micrographs of hBN containing EG-water mixture nanofluids presented in Figure 3.9(b) shows similarity to poly-dispersed state with small cluster formations, the particle distribution pattern does not lead to a highly effective conductive mechanism. This also suggests that the percolation through the loose chain structures is also supported by Brownian motion in water based nanofluids, which is limited for water/EG based nanofluids due to increased base fluid viscosity. The thermal conductivity enhancement is approximately 7.7% for 1% particle loading and increases up to 22% for 3% particle loading. A similar result can also be seen for EG based nanofluids. No significant thermal conductivity enhancement for diluted concentrations can be observed in Figure 3.10. While about 2.2% thermal conductivity enhancement that is beyond measurement uncertainty is observed for 0.5% particle volume concentration, for 1% particle volume concentration enhancement increases to 6.7%, and for 3% particle volume concentration it further increases to 16%. The observed steady, monotonically increasing trend can be explained with the dispersion state of EG-hBN nanofluids. Observing the micrographs of hBN-EG nanofluids presented in Figure 3.9(a), it can be seen that nanoparticles are not forming local clusters and they are almost evenly distributed in the liquid media. Considering that the local percolation mechanism is the dominant cause for heat transfer enhancement in hBN-water nanofluids, thermal conductivity enhancement of hBN-EG nanofluids is limited as formation of local clusters are hindered. The thermal conductivity of hBN–EG/water nanofluid can be represented as:

$$\frac{k_{nf}}{k_{bf}} = -96\varphi^2 + 10.5\varphi + 1 \tag{3.3}$$

whereas, the thermal conductivity of hBN–EG nanofluid can be represented as:

$$\frac{k_{nf}}{k_{bf}} = -21\varphi^2 + 5.63\varphi + 1 \tag{3.4}$$

It can be summarized that water based nanofluids, with their distinctive poly-dispersed state and local interconnecting particle alignment, demonstrate superior thermal conductivity increase starting from diluted concentrations compared to other types of base fluids. Even though EG/water based nanofluids do not demonstrate any significant increment at diluted concentrations, they exhibit thermal conductivity enhancement superior to EG based nanofluids and such behavior can be attributed to limited percolating cluster formations where the EG based nanofluids lack of with their almost mono-dispersed state.

3.5. Viscosity of Nanofluids

Following thermal conductivity enhancement, rheological behavior of the hBN nanofluids is investigated. It was observed that all the water-hBN nanofluid samples exhibit Newtonian behavior. Figure 3.12. presents rheological behavior of 1, 2 and 3% hBN-water nanofluids, for the shear rate range of 375-1850 s^{-1}. EG-water (50% by volume) based nanofluids exhibit Newtonian behavior between shear rates of 30-400 s^{-1}. EG based nanofluids are tested under a relatively smaller shear rate range between 20-160 s^{-1} and demonstrated Newtonian behavior.

As can be observed in Figure 3.13., viscosity increase in hBN-water nanofluids is relatively lower (up to 5%) than the thermal conductivity increase for dilute concentrations ($\varphi \leq 0.1\%$). For higher concentrations, nanofluid to base fluid viscosity ratio increases up to 22% for nanofluids containing 3% hBN by volume. It can be stated that compared to that of thermal conductivity increase in hBN-water nanofluids, viscosity increase is slightly smaller. Viscosity increase is larger for hBN-EG nanofluids and leads up to 33% increase for 3 % particle volume concentration. The largest increase is observed for hBN-water/EG nanofluids with 62% for 3% particle volume concentration. It can be clearly seen that only water based nanofluids demonstrate a viscosity increase that is not larger than the thermal conductivity enhancement. The equations representing hBN nanofluids' viscosity with

respect to their particle volume concentration can be derived through a polynomial fit. For hBN–water nanofluids the equation is:

$$\frac{\mu_{nf}}{\mu_{bf}} = -96\varphi^2 + 4.43\varphi + 1 \tag{3.5}$$

For hBN–EG/water nanofluids:

$$\frac{\mu_{nf}}{\mu_{bf}} = 3080\varphi^2 + 10.98\varphi + 1 \tag{3.6}$$

and hBN–EG nanofluids:

$$\frac{\mu_{nf}}{\mu_{bf}} = 15\varphi^2 + 11.47\varphi + 1 \tag{3.7}$$

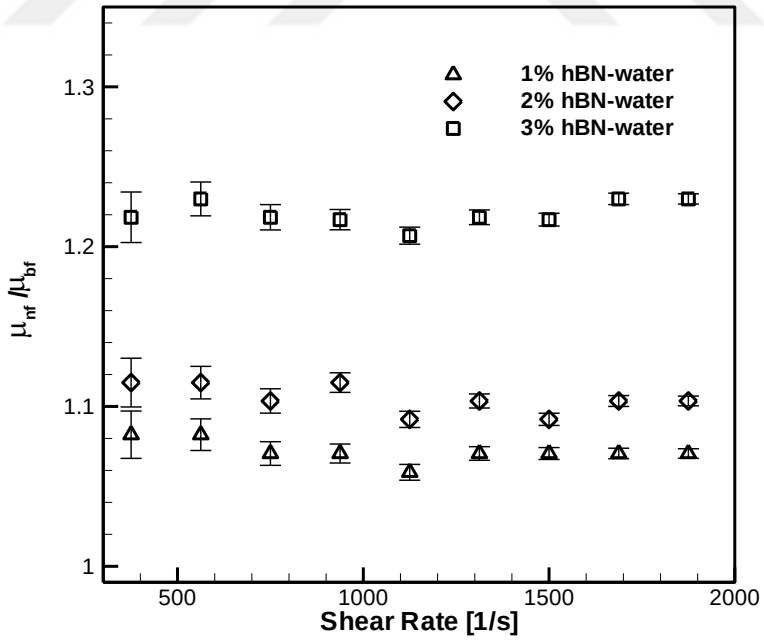

Figure 3.12. Rheological behavior of water-hBN nanofluids 1-3% particle volume concentration.

Presented viscosity increases are compared with several correlations including Einstein model (1905) for particle loadings up to 2%, Brinkman model (1947) and Corcione model (2012) for each different base fluid type. While Einstein and Brinkman models underestimates the viscosity change for all nanofluids, Corcione model predicts water based nanofluids' viscosity increase reasonably well. Although Corcione model underestimates EG and EG/water based nanofluids' viscosity increase, it should be noted that all the nanofluids contain both hBN-nanoparticles and surfactant materials, SDS or PVP, in different amounts. Besides, it was shown that adding these surfactant materials to base fluids have insignificant effect on thermal conductivity, whereas they introduce an increase in viscosity of the base fluid. Therefore, using surfactant added base fluid's viscosity improves the prediction accuracy of EG based nanofluids' viscosity to a reasonable level when Corcione correlation is used. However, the model still underestimates viscosity increase for EG/water based nanofluids if similar approach is used.

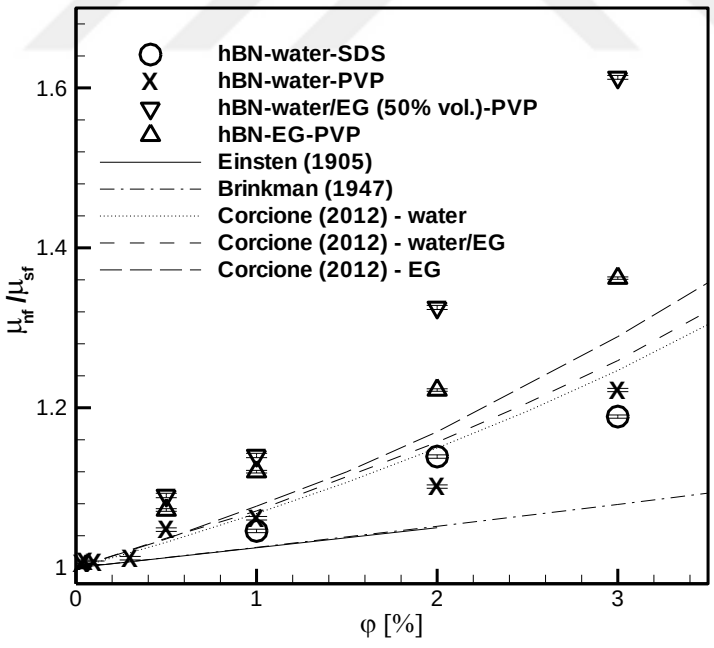

Figure 3.13. Change in nanofluid to base fluid viscosity ratio of hBN nanofluids.

3.6. Convective Heat Transfer of Nanofluids

Before conducting the experiments on nanofluids, the constructed test setup is validated with consecutive experiments by using deionized (DI) water at different Reynolds numbers. For the validation study, the measured quantities are compared to the estimations based on correlation by Churchill and Ozoe (1973). The measured and predicted local heat transfer coefficients for thermally developing, laminar, forced convection of water subjected to uniform heat flux for Reynolds numbers of 1200 and 1600 are presented in Figure 3.14. Results indicate that there is a reasonable agreement between the theoretical predictions and experimental values within the range of measurement uncertainty. Similar comparisons are also carried out for a broad range of Reynolds numbers, and complementary agreements are observed.

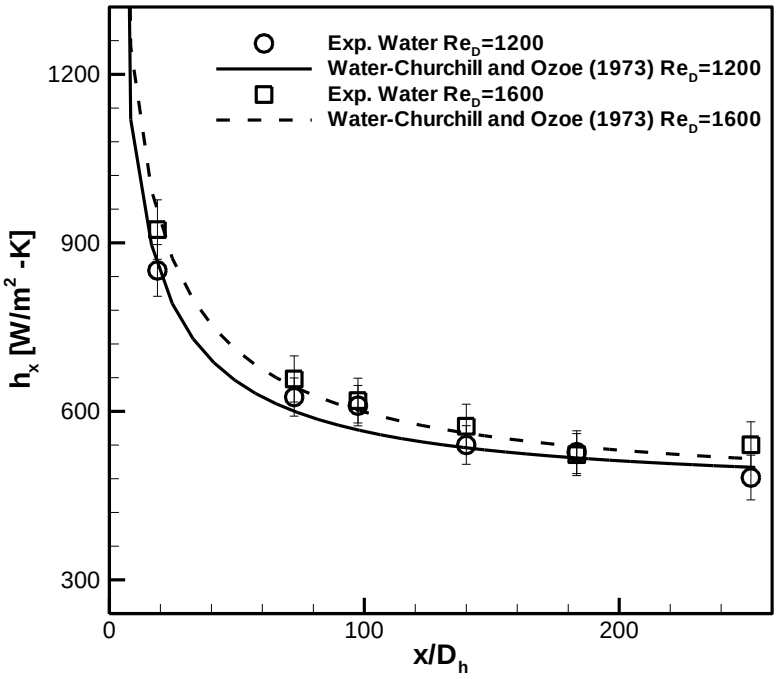

Figure 3.14. Comparison of experimental local heat transfer coefficient and predictions from theoretical correlation by Churchill and Ozoe (1973) for Re=1200 and 1600 for DI water

Following the validation of the measurement setup, systematic experiments are conducted over a Reynolds number range of 800-1700 with hBN-water nanofluids with

different particle volume concentrations. The experiments at the corresponding Reynolds numbers (±50) are first conducted with DI water to establish a baseline measurement, and investigate enhancement with respect to it.

The change in the local heat transfer coefficient along the axial direction for nanofluids with 3 different hBN volume fractions, 0.1%, 0.5%, 1%, are presented in Figure 3.15. for Reynolds numbers of 900 and 1700, respectively. While heat transfer coefficient increases with increasing particle loading, the rate of enhancement with respect to base fluid seems to be similar throughout the developing region. Moreover, as a distinctive remark, the enhancement is independent of Reynolds number. The heat transfer enhancement is approximately 7, 10, 15% for volume concentrations of 0.1, 0.5 and 1%, respectively, which is similar to thermal conductivity enhancement observed in Figure 3.10. This is also clearly observed when the predictions of local heat transfer coefficient along axial direction by the Churchill and Ozoe correlation are compared to measurements.

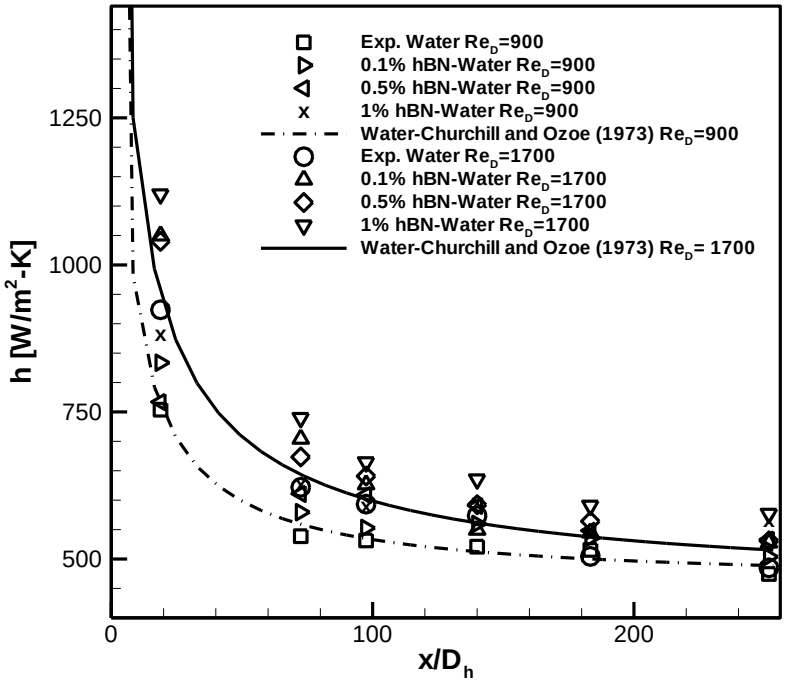

Figure 3.15. 0.1, 0.5, 1 % hBN-water nanofluids' local heat transfer coefficient change along the axial direction for Re_D= 900 and 1700

The changes in the local heat transfer coefficient along the axial distance for nanofluids with 0.5% hBN volume concentration at Reynolds numbers of 800, 1200 and 1600 are presented along with predictions from the Churchill-Ozoe correlation in Figure. 3.16. It can be observed that measured results are in good agreement with the predictions by the correlation, and the enhancement in the heat transfer coefficient is similar to thermal conductivity enhancement for the prescribed volume fraction.

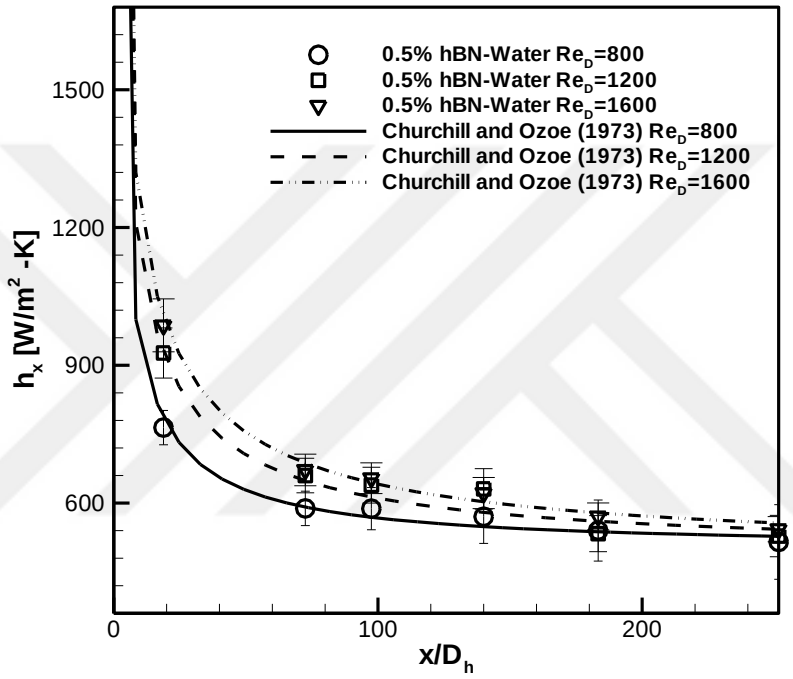

Figure 3.16. Comparison between experimental values of 0.5% hBN nanofluid's local heat transfer coefficient and theoretical predictions from theoretical correlation by Churchill and Ozoe (1973) at Re_D=800,1200,1600

Similar conclusions can also be drawn from Figure 3.17., where local Nusselt number change for the same nanofluids with same Reynolds numbers of 900 and 1700 are presented. While no increasing trend can be observed with increased particle loading, all measured values fall within measurement uncertainty range of predictions of Churchill and Ozoe (1973) correlation. These results confirm that the observed enhancement in convective heat transfer is mainly due to increasing thermal conductivity and there is no apparent additional mechanism that contributes to the heat transfer enhancement

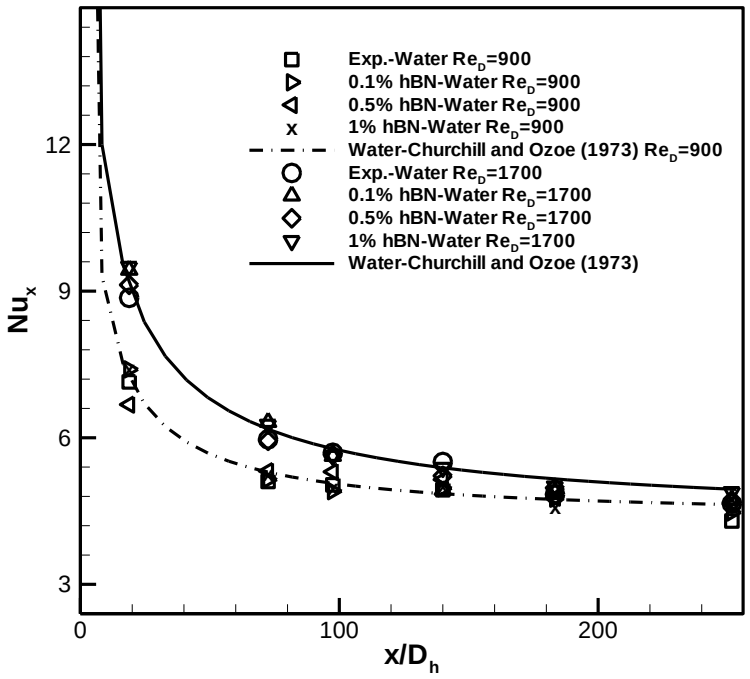

Figure 3.17. 0.1, 0.5, 1 % hBN-water nanofluids' local Nusselt number change along the axial direction for Re_D= 1700 and 900

Although the heat transfer enhancement with respect to base fluid does not change with changing Reynolds number (Fig. 3.16), the local heat transfer coefficient at a given axial location changes with Reynolds number for developing flow. The change in local heat transfer coefficient at two different axial locations, x/D_h=18.8 and x/D_h=251, is presented in Figure 3.18. for Reynolds numbers varying between 800 and 1700. The presented results are consistent with theory and more pronounced increase is observed at the entrance than as the flow develops as expected.

The complete data set is presented in Figure 3.19. that confirms the observations outlined earlier. Based on this, the convection heat transfer enhancement for the hBN-water nanofluids is due to the increase in thermal conductivity and there is no additional heat transfer enhancement mechanism is observed. Therefore, for laminar thermally developing flows theoretical correlations can be used to predict the heat transfer behavior.

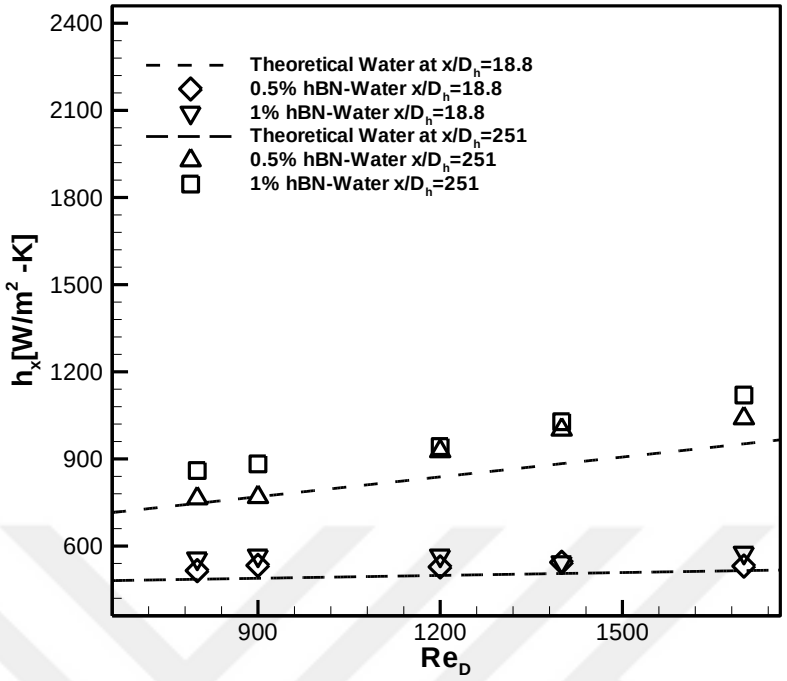

Figure 3.18. Nanofluid local heat transfer coefficient change with Reynolds number at 2 different axial locations, (x/D_h=18.8 and 251)

Considering the obtained results in this study, it can be clearly said that for the laminar flow regime hBN-water nanofluids demonstrate increase in the convective heat transfer behavior, that is proportional to that of thermal conductivity. Major outcome that can be infered from such results is that hBN-water nanofluids demonstrates convective heat transfer characteristics of homogenous mixtures, leading no abnormal change. Different thermophysical properties of such nanofluids with respect to water results in a predictable change in convective heat transfer behavior with no significant change in dimensionless Nusselt number beyond the measurement uncertainities. Considering the remark that is interfered from thermal conductivity enhancement results of hBN-water nanofluids, the enhancement mechanism behind the thermal properties of such nanofluids can be considered as predominantly the local percolating structures. As observed from the convective heat transfer experiments' results, there is no other mechanism behind the convective heat transfer other than that of thermal conductivity enhancement's. Although there is a variety of data presented in literature for outlining the convective heat transfer behavior of nanofluids, as stated in the previous sections, there is no consensus among the superior characteristics of nanofluids in terms of convective heat transfer. In accordance with our results, Sommers and Yerkes (2010) worked with propanol nanofluids containing

Al_2O_3 nanoparticles and they stated that the observed enhancement in convective heat transfer can be attributed to the change in the thermophysical property change within the nanofluids. They stated that there is no abnormal change in convective heat transfer characteristics and so that the dimensionless parameter, $Nu/Pr^{1/3}$, remains with no significant change. Rea *et al.* (2008) worked with Al_2O_3-water nanofluids and claimed that within the range of volume concentration between 0.65%-1.32% there is no abnormal change in convective heat transfer beyond the experimental uncertainty limits. Similar results stating that the change in convective heat transfer characteristics can be dominantly dependent on the thermophysical property change of nanofluids can also be seen in literature (Williams *et al.*, 2008; Wang and Mujumdar, 2007, Prabhat *et al.* 2011).

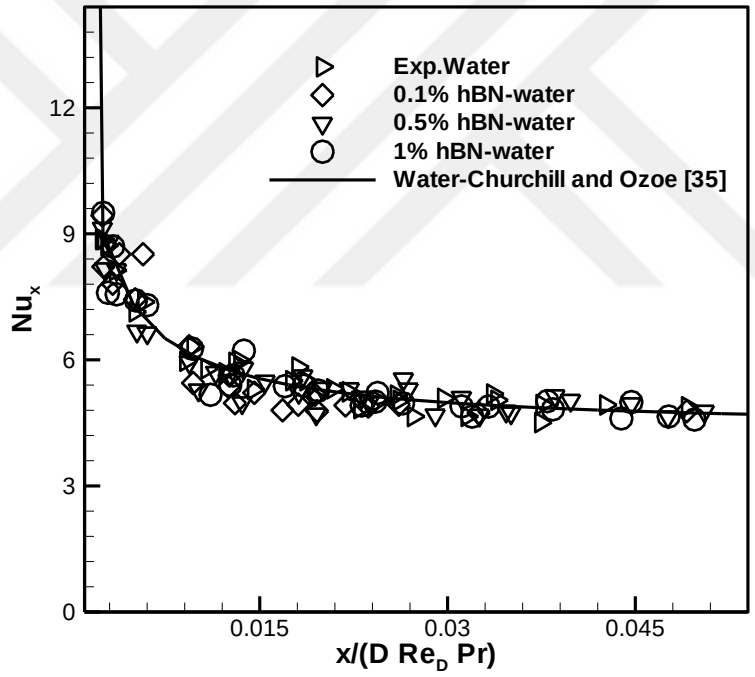

Figure 3.19. The change in the all experimental Nusselt number along the test section

One of the major outcomes that should be noted here is that all the sample nanofluids' thermal conductivity and viscosity values are measured before and after the experiments and samples are kept to further investigate their temporal stability. Results show that thermophysical properties of such nanofluids remains identical with high level of stability even after the tests. It can be concluded that identified nanofluids in this study

are good candidates for future thermal engineering applications with their temporaly stable properties, making them effectively useful for reusable implementations.

4. CONCLUSION AND FUTURE WORK

4.1. Conclusion

Experimental studies for water, EG and EG/water mixture (50% by volume) based hBN nanofluids to characterize stability, investigate thermal, rheological and convective heat transfer behaviors are conducted for different volume concentrations varying between 0.03-3%.

Preparation procedures for all types of nanofluids are presented in detail. Although dry forms of hBN nanoparticles are forming agglomerations up to 4 times larger than the expected size (70 nm), DLS results show that by using the prescribed preparation recipe, particle sizes can be reduced to approximately 50 nm regardless of base fluid type. Two different surfactants, SDS and PVP, are used during two step preparation procedure of nanofluids. Although SDS provides an acceptable level of stability with water based nanofluids, due to excessive foaming and its failure to provide stability for EG and EG/water nanofluids, stable dispersions of hBN nanoparticles are achieved by using PVP. Considering stability as a thermal property relied metric, a contemporary way of determining nanofluids' stability is introduced as temporal thermal conductivity measurements. It is found that nanofluids with 1% particle volume concentration exhibit long term stability (more than 10 days) and stability duration of nanofluids with volume concentrations higher than 1% can be improved with optimizing surfactant material and amount. Morphological characterization of nanofluids are conducted with STEM imaging method and it is observed that water and EG/water mixture based nanofluids are in a poly-dispersed state, containing local cluster formations and dynamic free particles together, whereas EG based nanofluids can be considered as mono-dispersed colloids, without cluster formations.

Thermal conductivity measurement results show that thermal conductivity increases with increasing particle volume concentration and the increase is beyond the prediction of effective medium theories for all the base fluid types. Also hBN nanoparticles shows a remarkable thermal conductivity increase for water based nanofluids

even for very dilute concentrations. Thermal conductivity changes nonlinearly with particle concentration. A sudden increase in the thermal conductivity is observed for dilute suspensions. However, the increase rate slows after a certain volume concentration (0.5%). Such behavior can be explained with the formation of observed clusters. The sharp increase at the relatively lower volume concentrations is due to initialization of poly-dispersed state, where dynamic particles and local clusters coexist. These cluster formations act as heat conducting paths, leading to local percolating structures. As the volume concentration of the particles increases, clusters become more populated and packing fraction increases. However, increasing the density of existing clusters is not as effective as creating new ones, leading to a decrease in rate of thermal conductivity increase. Similar distinctive pattern is not observed for both EG and EG/water based nanofluids, which do not exhibit any remarkable enhancement at lower concentrations. Thermal conductivity increase for the presented hBN nanofluids reaches up to 26%, 22% and 16% at volume concentrations of 3% for water, water/EG mixture and EG based nanofluids, respectively.

All the hBN nanofluids exhibit Newtonian behavior within their prescribed shear rates. Viscosity increase is up to 22% for water based nanofluids, which indicates that water based nanofluids' thermal conductivity increase exceeds the increase in the viscosity. EG and EG/water based nanofluids' viscosity increases 33% and 62%, respectively, which is larger than the increase in their thermal conductivity. Although base fluids' viscosity have a significant effect on nanofluids' viscosity, interaction among base fluid, surfactant and nanoparticles should also be considered in order to comment more accurately on viscosity increase.

Convective heat transfer characteristics of hBN-water nanofluids in laminar thermally developing forced flow subjected to uniform heat flux in a circular pipe is investigated experimentally. Stable hBN nanofluids with 3 different volume concentrations (0.1, 0.5, 1%) are prepared with two step method and thermophysical and morphological characterization of nanofluids are completed prior to convection heat transfer experiments. This study considers laminar flow regime with a Reynolds number range of 800-1700. Based on the presented results, heat transfer coefficient increases with particle loading, but there is no abnormal enhancement observed. It is found that at a

constant Reynolds number, the enhancement in the convective heat transfer coefficient is similar to the increase in thermal conductivity within measurement uncertainty. The heat transfer enhancement is approximately 7, 10, 15% for volume concentrations of 0.1, 0.5 and 1%, respectively and as a result there is no significant change in the corresponding dimensionless Nusselt numbers. Therefore, it was concluded that there is no apparent additional heat transfer enhancement mechanism other than those effecting thermal conductivity. It should be noted that at constant Reynolds number for the considered hBN-water nanofluids, flow rates are slower as the particle volume concentration increases. Therefore, the results suggest that using hBN-water nanofluids increases convective heat transfer even at slower flow rates.

Considering the presented findings here, hBN nanofluids are promising candidates for future engineering applications where heat transfer enhancement is required. It is possible to attain high levels of thermal conductivity with respect to the viscosity increase especially for water based nanofluids. This will enable the use of hBN nanofluids for convective heat transfer applications, especially considering the fact that properties of hBN-water nanofluids remain unchanged after subjected to convective heat transfer experiments. It is also observed that long term use of hBN nanofluids containing PVP is possible for applications where these nanofluids are used in conjunction with turbomachinery that has an effect similar to that of mechanical mixers

4.2. Recommendations for Future Work

This study outlines a generalized recipe for hBN containing nanofluids with 3 different base fluids (water, EG and water/EG mixture). Although high level stability duration for the considered nanofluid samples is attained with prescribed surfactant amounts, a further study can be carried out to propose different amounts of surfactants especially for volume concentrations larger than 2% in order to reach maximum duration for higher volume concentrations.

It is stated herein that 2 step method with ultrasonication and surfactant addition is adequate for preparing each of the different volume concentrations separately. A major extension for this study could be about improving the know-how of preparing nanofluids

with different volume concentrations from a single hBN-base fluid suspension (nanofluid0). Meaning that, nanofluid preparation can be simplified as first producing a nanofluid with higher particle loading and then obtaining diluted forms (ie; lower concentrations) with dilution process via base fluid introduction. If characterization of such nanofluids obtained by diluting the high concentration one can be carried out, it would make the preparation process easier to implement into the mass production and industry.

Possible mechanisms behind the significant thermal conductivity enhancement is investigated here and discussed results point out the dominant effect of percolating structures. Further investigation of enhancement mechanisms especially for water based hBN nanofluids can be carried out to clearly understand the underlying effect in terms of thermal enhancement. Temperature dependence of the nanofluids' thermal conductivity values should be investigated to understand the effect of temperature. If this study is extended with thermal conductivity measurements with an adequate temperature range, effect and dominance of the Brownian motion can be observed more clearly.

Convective heat transfer behavior of hBN nanofluids are investigated under the laminar flow with a specified Reynolds number range. Extensive investigation can be further completed to characterize the convective heat transfer of hBN nanofluids with different flow regimes such as transition to turbulence and turbulent flows. Furthermore effect of convective heat transfer on the nanofluids' morphology can be investigated by conducting STEM characterization experiments of tested samples so that the particle alignment patterns can be observed right after the test. Such information can provide insight to dominant enhancement mechanisms for convective heat transfer. In addition, flow behavior of nanofluids can be further characterized by conducting pressure drop experiments as an extension of this work.

REFERENCES

Ahuja, A., S., (1975), Augmentation of Heat Transport in Laminar Flow of Polystyrene Suspensions. I. Experiments and Results. Journal of Applied Physics 46(8):3408.

Akhavan-Zanjani, H., Saffar-Avval, M., Mansourkiaei, M., Sharif, F., & Ahadi, M. (2016). Experimental investigation of laminar forced convective heat transfer of Graphene-water nanofluid inside a circular tube. International Journal of Thermal Sciences, 100, 316–323. doi:10.1016/j.ijthermalsci.2015.10.003

Assael, M. J., Metaxa, I. N., Arvanitidis, J., Christofilos, D., & Lioutas, C. (2005). Thermal conductivity enhancement in aqueous suspensions of carbon multi-walled and double-walled nanotubes in the presence of two different dispersants. International Journal of Thermophysics, 26(3), 647-664.

Baby, T. T., & Ramaprabhu, S. (2011). Enhanced convective heat transfer using graphene dispersed nanofluids. Nanoscale Research Letters, 6(1), 289. doi:10.1186/1556-276X-6-289

Baby, Tessy Theres, and S. Ramaprabhu. (2010). Investigation of Thermal and Electrical Conductivity of Graphene Based Nanofluids. Journal of Applied Physics 108(12).

Buongiorno, J., Venerus, D. C., Prabhat, N., McKrell, T., Townsend, J., Christianson, R., ... & Leong, K. C. (2009). A benchmark study on the thermal conductivity of nanofluids. Journal of Applied Physics, 106(9), 094312.

Chandrasekar, M., S. Suresh, and a. Chandra Bose. (2010). Experimental Investigations and Theoretical Determination of Thermal Conductivity and Viscosity of Al_2O_3/water Nanofluid. Experimental Thermal and Fluid Science 34(2): 210–16.

Choi, S. U. S. (1995). Enhancing thermal conductivity of fluids with nanoparticles. ASME-Publications-Fed, 231, 99-106.

Chou, J. C., & Liao, L. P. (2005). Study on pH at the point of zero charge of TiO 2 pH ion-sensitive field effect transistor made by the sputtering method. Thin Solid Films, 476(1), 157-161.

Churchill, S. W. ve Ozoe, H. (1973). Correlations for laminar forced convection with uniform heating in flow over a plate and in developing and fully developed flow in a tube, Journal of Heat Transfer, 95(1), 78-84..

Consdensed Phase Thermochemistry Data, National Institute of Standards and Technology, http://webbook.nist.gov/cgi/cbook.cgi?ID=C10043115&Units=SI&Mask=2#Thermo-Condensed34. Kline, S. J., & McClintock, F. A. (1953). Describing uncertainties in single-sample experiments. Mechanical engineering, 75(1), 3-8.

Das, S. K., Choi, S. U. S., Yu, W., & Pradeep, T., (2007), Nanofluids: science and technology John Wiley & Sons.

Das, S. K., Choi, S. U., & Patel, H. E. (2006). Heat transfer in nanofluids—a review. Heat transfer engineering, 27(10), 3-19.

Das, S. K., Putra, N., Thiesen, P., & Roetzel, W. (2003). Temperature dependence of thermal conductivity enhancement for nanofluids. Journal of Heat Transfer, 125(4), 567-574.

Daungthongsuk, W., Wongwises, S. (2007). A critical review of convective heat transfer of nanofluids, Renewable and Sustainable Energy Reviews, 11(5), 797-817.

DeNardis, D., Choi, H., Kim, A., Moinpour, M., & Oehler, A. (2005, January). Investigating the effects of diluting solutions and trace metal contamination on aggregation characteristics of silica-based ILD CMP slurries. In MRS Proceedings (Vol. 867, pp. W7-9). Cambridge University Press.

Ding Y., Alias H., Wen D.,. Williams R., (2006). Heat Transfer of Aqueous Suspensions of Carbon Nanotubes (CNT Nanofluids). International Journal of Heat and Mass Transfer 49(1-2):240–50.

Eapen, J., Li, J., & Yip, S. (2007). Mechanism of thermal transport in dilute nanocolloids. Physical review letters, 98(2), 028302.

Eastman, J. A., Choi, U. S., Li, S., Thompson, L. J., & Lee, S. (1996). Enhanced thermal conductivity through the development of nanofluids. In MRS proceedings (Vol. 457, p. 3). Cambridge University Press.

Esmaeilzadeh, E., Almohammadi, H., Nasiri Vatan, S., & Omrani, A. N. (2013). Experimental investigation of hydrodynamics and heat transfer characteristics of γ-Al_2O_3/water under laminar flow inside a horizontal tube. International Journal of Thermal Sciences, 63, 31–37. doi:10.1016/j.ijthermalsci.2012.07.001

Gao, J. W., Zheng, R. T., Ohtani, H., Zhu, D. S., & Chen, G. (2009). Experimental investigation of heat conduction mechanisms in nanofluids. Clue on clustering. Nano letters, 9(12), 4128-4132.

Ghadimi, A., & Metselaar, I. H. (2013). The influence of surfactant and ultrasonic processing on improvement of stability, thermal conductivity and viscosity of titania nanofluid. Experimental Thermal and Fluid Science, 51, 1-9.

Ghadimi, A., Saidur, R., & Metselaar, H. S. C. (2011). A review of nanofluid stability properties and characterization in stationary conditions. International Journal of Heat and Mass Transfer, 54(17-18), 4051–4068.

Guo, J. F., Guo, Z. Q., Wang, X. F., Li, Y. J., & Lv, Q. J. (2015). Experimental Investigation on Thermophysical Performance of BN/EG Nanofluids Influenced by Dispersant. Applied Mechanics and Materials, 757, 7–12.

Gupta, M., Arora, N., Kumar, R., Kumar, S., & Dilbaghi, N. (2014). A comprehensive review of experimental investigations of forced convective heat transfer characteristics for various nanofluids, 1–21. doi:10.1186/s40712-014-0011-x

Haghighi, E B *et al.* (2013). Shelf Stability of Nanofluids and Its Effect on Thermal Conductivity and Viscosity. Measurement Science and Technology 24(10): 105301.

Hemmat Esfe, M., Saedodin, S., Mahian, O., & Wongwises, S. (2014). Heat transfer characteristics and pressure drop of of COOH-functionalized DWCNTs/water nanofluid in turbulent flow at low concentrations. International Journal of Heat and Mass Transfer, 73, 186–194. doi:10.1016/j.ijheatmasstransfer.2014.01.069

Huang, J., Wang, X., Long, Q., Wen, X., Zhou, Y., & Li, L. (2009, August). Influence of pH on the stability characteristics of nanofluids. In Photonics and Optoelectronics, 2009. SOPO 2009. Symposium on (pp. 1-4). IEEE.

Hwang, K. S., Jang S. P., Choi S. U. S., (2009), Flow and Convective Heat Transfer Characteristics of Water-Based Al_2O_3 Nanofluids in Fully Developed Laminar Flow Regime. International Journal of Heat and Mass Transfer 52(1-2):193–99.

İlhan, B., Kurt, M., & Ertürk, H. (2016). Experimental investigation of heat transfer enhancement and viscosity change of hBN nanofluids. Experimental Thermal and Fluid Science, 77, 272-283.

Jang, S. P., & Choi, S. U. (2004). Role of Brownian motion in the enhanced thermal conductivity of nanofluids. Applied physics letters, 84(21), 4316-4318.

Kabelac, S., & Kuhnke, J. F., (2006), Heat transfer mechanism in nanofluids-Experiments and theory, International Heat Transfer Conference 13. Begel House Inc.

Karthikeyan, N. R., Philip, J., & Raj, B. (2008). Effect of clustering on the thermal conductivity of nanofluids. Materials Chemistry and Physics, 109(1), 50-55.

Keblinski, P, S R Phillpot, S U S Choi, and J A Eastman. (2002). Mechanisms of Heat Flow in Suspensions of Nano-Sized Particles (Nano Fluids). 45: 855–63.

Kim, N. J., Park, S. S., Lim, S. H., & Chun, W. (2011). A study on the characteristics of carbon nanofluids at the room temperature (25° C). International Communications in Heat and Mass Transfer, 38(3), 313-318.

Kline, S. J., & McClintock, F. A. (1953). Describing uncertainties in single-sample experiments. Mechanical engineering, 75(1), 3-8.

Lee, D., Kim, J. W., & Kim, B. G. (2006). A new parameter to control heat transport in nanofluids: surface charge state of the particle in suspension. The Journal of Physical Chemistry B, 110(9), 4323-4328.

Lee, J. H., Hwang, K. S., Jang, S. P., Lee, B. H., Kim, J. H., Choi, S. U., & Choi, C. J. (2008). Effective viscosities and thermal conductivities of aqueous nanofluids containing low volume concentrations of Al_2O_3 nanoparticles. International Journal of Heat and Mass Transfer, 51(11), 2651-2656.

Lee, S., S. U.-S. Choi, S. Li, and J. a. Eastman. (1999). Measuring Thermal Conductivity of Fluids Containing Oxide Nanoparticles. Journal of Heat Transfer 121(2): 280.

Li, Y., Zhou, J., Luo, Z., Tung, S., Schneider, E., Wu, J., & Li, X. (2011). Investigation on two abnormal phenomena about thermal conductivity enhancement of BN/EG nanofluids. Nanoscale Research Letters, 6(1), 443.

Mohan, M., Thomas, S., Taha-Tijerina, J., Narayanan, T. N., Sobhan, C. B., & Ajayan, P. M. (2013, November). Heat Transfer Studies in Thermally Conducting and Electrically Insulating Nano-Oils in a Natural Circulation Loop. In ASME 2013 International Mechanical Engineering Congress and Exposition (pp. V06BT07A040-V06BT07A040). American Society of Mechanical Engineers.

Murshed, S. M. S., Leong, K. C., & Yang, C. (2008). Investigations of thermal conductivity and viscosity of nanofluids. International Journal of Thermal Sciences, 47(5), 560-568.

Murshed, S.M. Sohel, and C.a. Nieto de Castro. (2014). Superior Thermal Features of Carbon Nanotubes-Based Nanofluids – A Review. Renewable and Sustainable Energy Reviews 37: 155–67.

Nikkam, N., Ghanbarpour, M., Saleemi, M., Haghighi, E. B., Khodabandeh, R., Muhammed, M., ... & Toprak, M. S. (2014). Experimental investigation on thermo-physical properties of copper/diethylene glycol nanofluids fabricated via microwave-assisted route. Applied Thermal Engineering, 65(1), 158-165.

Patel, H. E., Anoop, K. B., Sundararajan, T., & Das, S. K. (2006). A micro-convection model for thermal conductivity of nanofluids. In International Heat Transfer Conference 13. Begel House Inc..

Perez-Maqueda, L. A., J. M. Blanes, J. Pascual, J. L. Perez-Rodriguez, (2004), The Influence of Sonication on the Thermal Behavior of Muscovite and Biotite, Journal of the European Ceramic Society, Vol. 24, No. 9, pp. 2793-2801.

Prasher, R., Phelan, P. E., & Bhattacharya, P. (2006). Effect of aggregation kinetics on the thermal conductivity of nanoscale colloidal solutions (nanofluid). Nano Letters, 6(7), 1529-1534.

Rayatzadeh, H. R., Saffar-Avval, M., Mansourkiaei, M., & Abbassi, A. (2013). Effects of continuous sonication on laminar convective heat transfer inside a tube using water-TiO_2 nanofluid. Experimental Thermal and Fluid Science, 48, 8–14. doi:10.1016/j.expthermflusci.2013.01.016

Rea, U., McKrell T., Hu L., & Buongiorno J., (2009), Laminar Convective Heat Transfer and Viscous Pressure Loss of Alumina–water and Zirconia–water Nanofluids. International Journal of Heat and Mass Transfer 52(7-8):2042–48.

Sahoo, R. R., Bhattacharjee, S., & Das, T. (2013). Development of Nanofluids As Lubricant To Study Friction and Wear Behavior of Stainless Steels. International Journal of Modern Physics: Conference Series, 22, 664–669.

Sleiti, A. K. (2013). Experimental Measurement of Viscosity of Boron Nitride-Polyalpha Olefin Nanofluid, 02(2005), 330–334.

Sleiti, A. K., (2011), "Rheological Characteristics of Boron Nitride Nanofluids with Polyalpha-Olein Oil Base Fluid", Proceedings of IMECE 2011, Denver, Colorado, USA.

Sohn, Cw, and Mm Chen. (1981). Microconvective Thermal Conductivity in Disperse Two-Phase Mixtures as Observed in a Low Velocity Couette Flow Experiment. Journal of Heat Transfer 103(February 1981): 47–51.

Sommers, A., D., Yerkes K. L., (2010), Experimental Investigation into the Convective Heat Transfer and System-Level Effects of Al_2O_3-Propanol Nanofluid. Journal of Nanoparticle Research 12:1003–14.

Studart, A. R., Amstad, E., & Gauckler, L. J. (2007). Colloidal stabilization of nanoparticles in concentrated suspensions. Langmuir, 23(3), 1081-1090.

Taha-Tijerina, J., Narayanan, T. N., Gao, G., Rohde, M., Tsentalovich, D. a, Pasquali, M., & Ajayan, P. M. (2012). Electrically insulating thermal nano-oils using 2D fillers. ACS Nano, 6(2), 1214–20.

Taha-Tijerina, J., Peña-Paras, L., Narayanan, T. N., Garza, L., Lapray, C., Gonzalez, J., … Ajayan, P. M. (2013). Multifunctional nanofluids with 2D nanosheets for thermal and tribological management. Wear, 302(1-2), 1241–1248.

Timofeeva, Elena *et al.* (2007). Thermal Conductivity and Particle Agglomeration in Alumina Nanofluids: Experiment and Theory. Physical Review E 76(6): 061203.

Wang, J., Zhu, J., Zhang, X., & Chen, Y. (2013). Heat transfer and pressure drop of nanofluids containing carbon nanotubes in laminar flows. Experimental Thermal and Fluid Science, 44, 716–721. doi:10.1016/j.expthermflusci.2012.09.013

Wang, J.J., R.T. Zheng, J.W. Gao, and G. Chen. (2012). Heat Conduction Mechanisms in Nanofluids and Suspensions. Nano Today 7(2): 124–36.

Wang, X. Q., Mujumdar, A. S. (2007). Heat transfer characteristics of nanofluids: a review, International journal of thermal sciences, 46(1), 1-19.

Wang, X. Q., & Mujumdar, A. S. (2008). A review on nanofluids-part II: experiments and applications. Brazilian Journal of Chemical Engineering, 25(4), 631-648.

Wen, D., & Yulong D., (2004), Experimental Investigation into Convective Heat Transfer of Nanofluids at the Entrance Region under Laminar Flow Conditions. International Journal of Heat and Mass Transfer 47(24):5181–88.

Wong, K. V., & Castillo, M. J. (2010). Heat Transfer Mechanisms and Clustering in Nanofluids. Advances in Mechanical Engineering, 2010, 1–9.

Xie, H., Wang, J., Xi, T., & Liu, Y. (2001). Study on the thermal conductivity of SiC nanofluids. J. Chin. Ceram. Soc., 29(4), 361-364.

Xuan, Y., Li, Q., & Tie, P. (2013). The effect of surfactants on heat transfer feature of nanofluids. Experimental Thermal and Fluid Science, 46, 259-262.

Yang, Y., Grulke, E. A., Zhang, Z. G., & Wu, G. (2006). Thermal and rheological properties of carbon nanotube-in-oil dispersions. Journal of Applied Physics, 99(11), 114307.

Yu, W., & Xie, H. (2012). A review on nanofluids: preparation, stability mechanisms, and applications. Journal of Nanomaterials, 2012, 1.

Zhi, C., Xu, Y., Bando, Y., & Golberg, D. (2011). Highly Thermo-conductive Fluid with Boron Nitride Nano fi llers, (8), 6571–6577.

Zhou M. *et al.* (2012). Analysis of Factors Influencing Thermal Conductivity and Viscosity in Different Kinds of Surfactant Solutions. Experimental Thermal and Fluid Science 36: 22–29.

Zhu, H., Zhang, C., Liu, S., Tang, Y., & Yin, Y. (2006). Effects of nanoparticle clustering and alignment on thermal conductivities of Fe3O4 aqueous nanofluids. Applied Physics Letters, 89(2), 3123.

Żyła, G., Witek, A., & Gizowska, M. (2015). Rheological profile of boron nitride–ethylene glycol nanofluids. Journal of Applied Physics, 117(1), 01430

APPENDIX A: MICROGRAPH IMAGES FOR hBN NANOFLUIDS

A.1. 0.1% hBN-Water Nanofluids

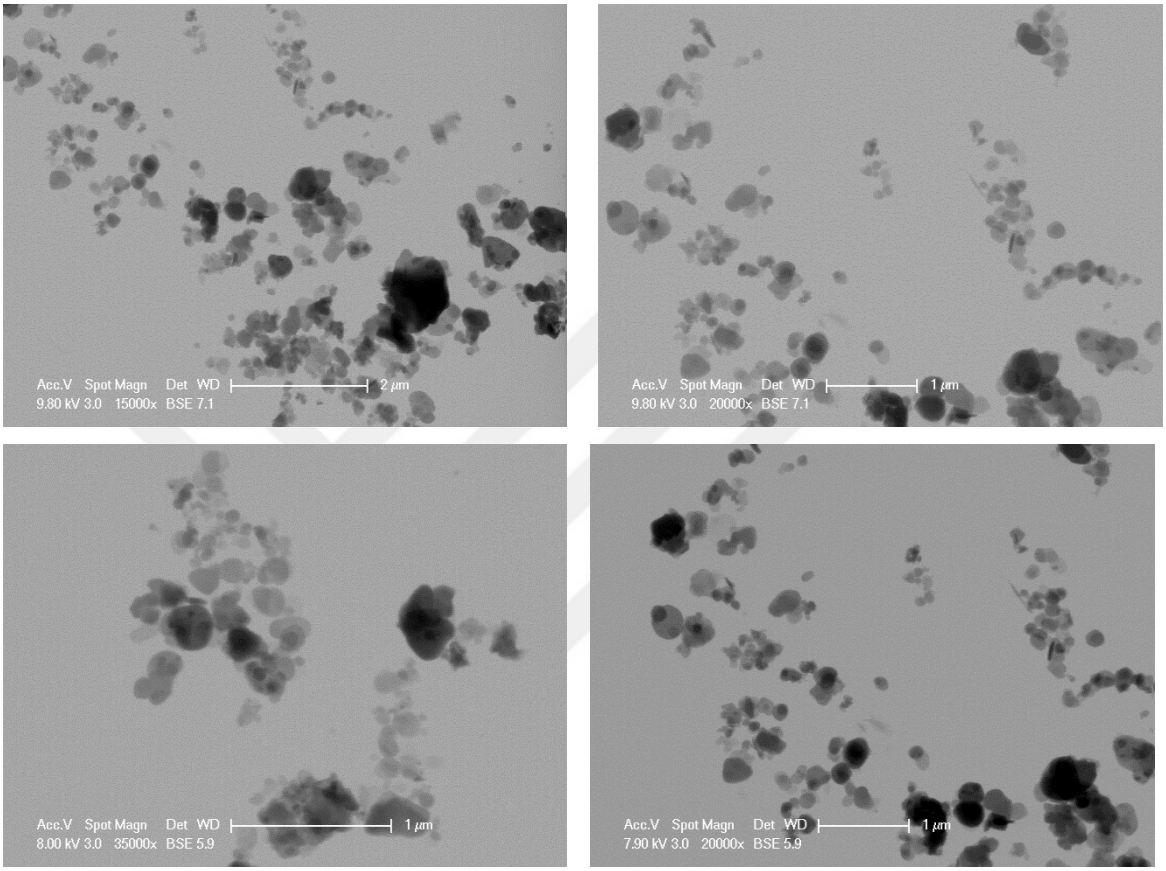

Figure A.1. 0.1% hBN-water nanofluid samples' STEM images

A.2. 0.5% hBN-Water Nanofluids

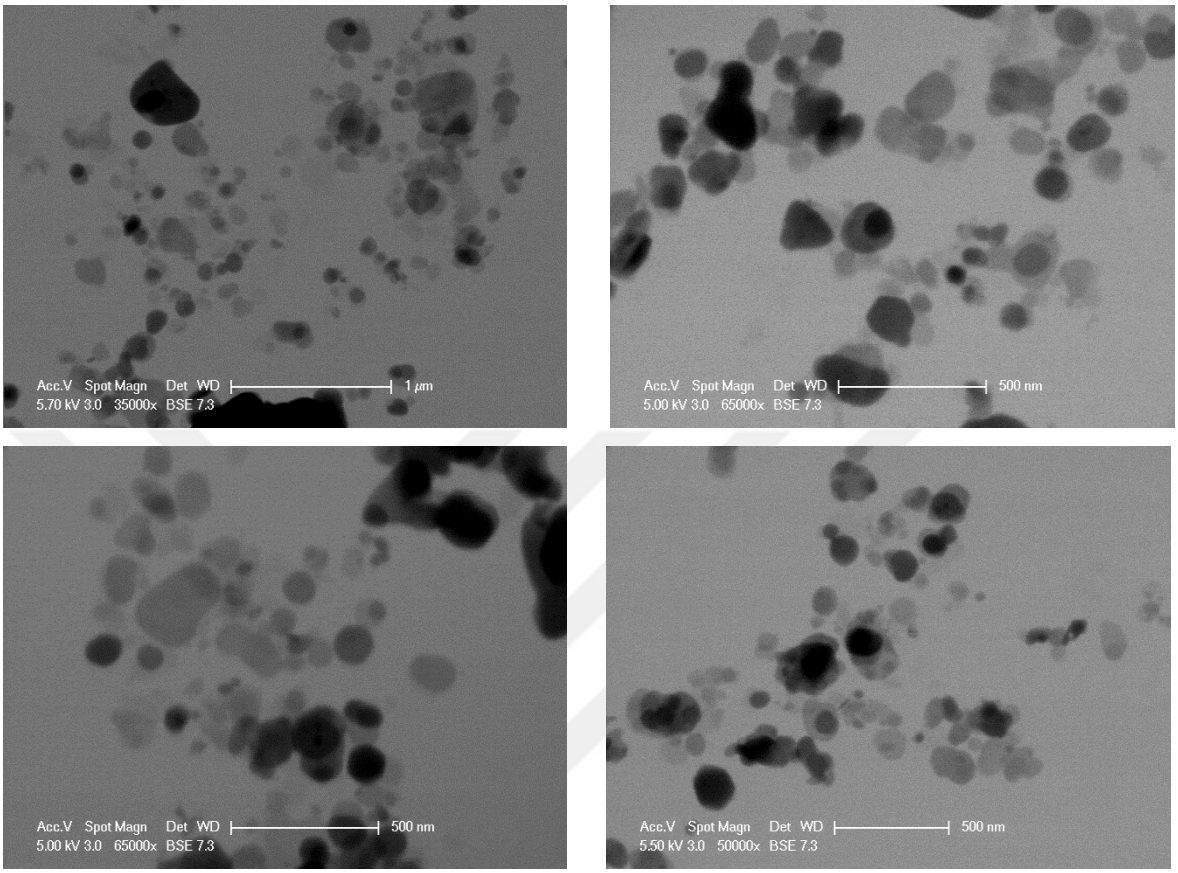

Figure A.2. 0.5% hBN-water nanofluid samples' STEM images

A.3. 2% hBN-Water Nanofluids

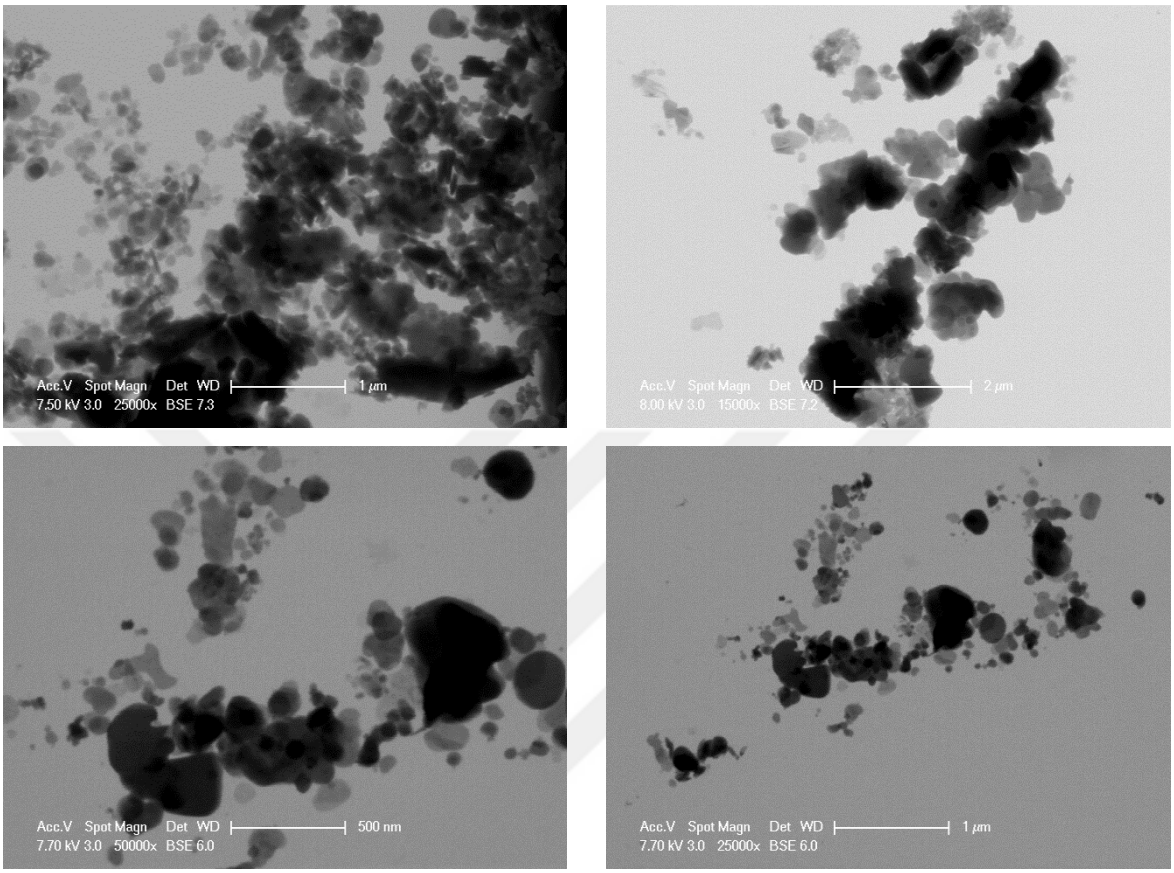

Figure A.3. 2% hBN-water nanofluid samples' STEM images

A.4. 0.5% hBN-EG/Water Nanofluids

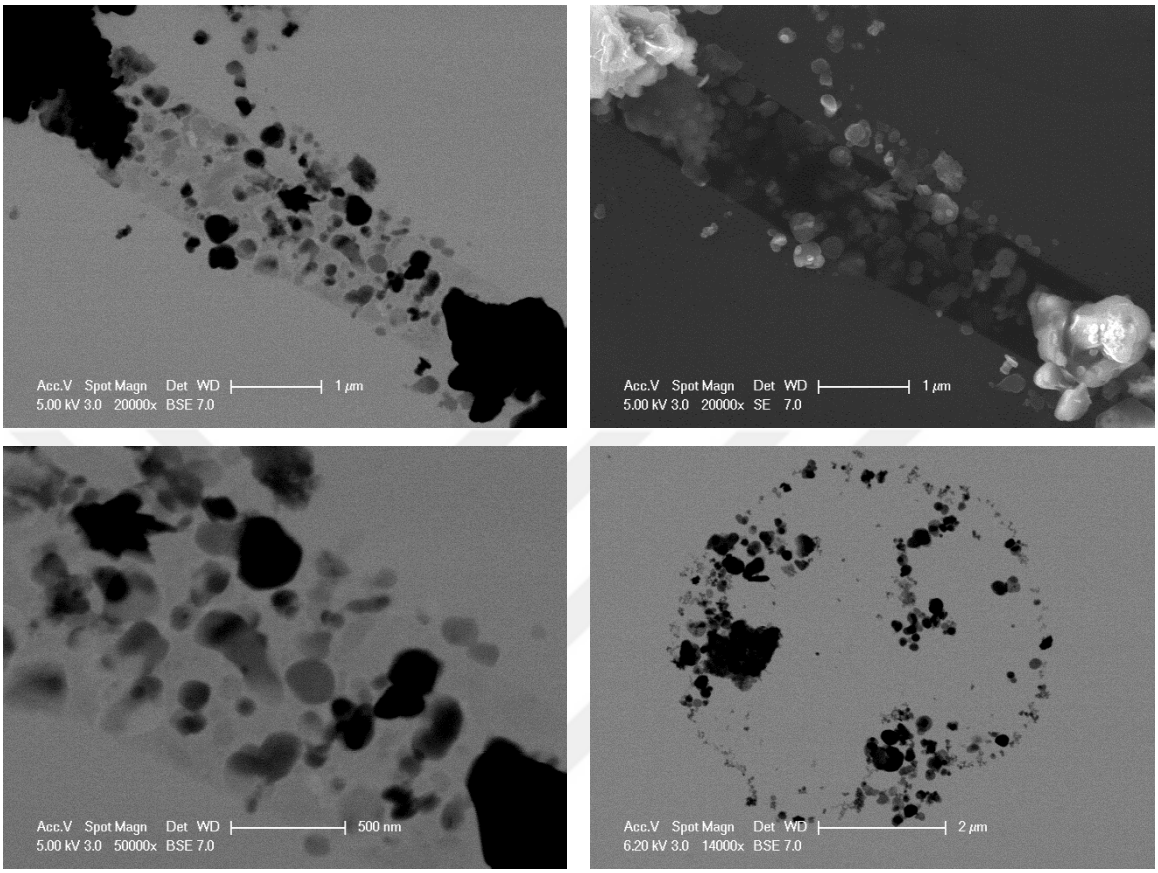

Figure A.4. 0.5% hBN-EG/water nanofluid samples' STEM and ESEM images